HUNTING NEW ANIMALCULA WITH FLAVOUR CHANGING PROCESSES*

Andrzej J. Buras

TUM Institute for Advanced Study
Lichtenbergstraße 2a, 85748 Garching, Germany
and
Physik Department, TUM School of Natural Sciences, TU München
James-Franck-Straße, 85748 Garching, Germany
aburas@ph.tum.de

Received 13 May 2026, accepted 13 May 2026, published online 28 May 2026

This year marks the 350th anniversary of the discovery of the first animalcula (little animals) by van Leeuwenhoek in 1676. Flavour physics makes it possible to search for new animalcula at distance scales far shorter than those resolved by van Leeuwenhoek in 1676, and even shorter than those directly accessible at the Large Hadron Collider and the planned colliders in this century. I summarize various strategies for achieving this goal. While precise measurements of a wide variety of observables and their precise theoretical calculations, both within the Standard Model (SM) and beyond it, are indispensable in this context, in my view, it is crucial to develop strategies for the search for New Physics (NP) that go beyond the global fits that are very popular today. While effective field theories such as WET and SMEFT are formulated in terms of Wilson coefficients of the relevant operators, with correlations characteristic of the SM and of specific NP scenarios, the most direct tests of the SM and its extensions are, in my opinion, correlations among different observables, like branching ratios of numerous decays, that are characteristic of particular new animalcula at work.

DOI:10.5506/APhysPolB.57.6-A15

1. Overture and outline

The year 2026 is rather special for those who study short-distance scales. It marks the 350th anniversary of the discovery of the empire of bacteria made in 1676 by Antoni van Leeuwenhoek (1632–1723) (See Fig. 1). He called these small creatures *animalcula* (little animals). This discovery was a milestone in our civilization for several reasons. He discovered invisible to us creatures which over thousands of years were systematically killing

the humans, often responsible for millions of deaths in one year. While Antoni van Leeuwenhoek and his important follower Lazzaro Spallanzani (1729–1799) did not realize the danger coming from these new living species, fortunately, Louis Pasteur (1822–1895) and Robert Koch (1843–1910) as well as other *microbe hunters* not only realized the danger coming from these tiny creatures but also developed weapons against this empire[1]. Moreover, van Leeuwenhoek was the first human who looked at short-distance scales invisible to us, discovering thereby a new *underground world: microuniverse*.

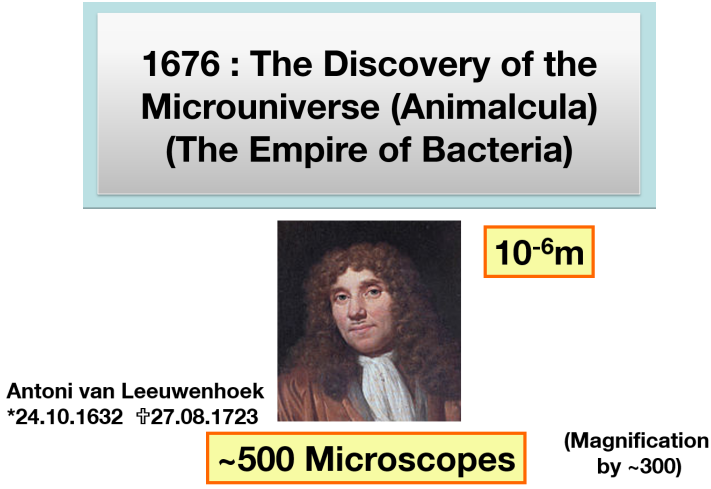

Fig. 1. Antoni van Leeuwenhoek. (Wikipedia)

While van Leeuwenhoek could reach the resolution down to roughly 10^{-6} m, over the last 350 years, this resolution could be improved by many orders of magnitude reaching already in 1980 the resolution of 10^{-15} m in the context of low-energy elementary particle physics. As seen in Fig. 2, it has further been improved by many orders of magnitude since then.

On the way down to the shortest-distance scales, scientists discovered the *nanouniverse* (10^{-9} m), the *femtouniverse* (10^{-15} m) relevant for nuclear particle physics and low-energy elementary particle physics, and finally, the *attouniverse* (10^{-18} m) that is the territory of contemporary high-energy elementary particle physics.

In this decade and the coming decades, we will be able to improve the resolution of the short-distance scales by at least an order of magnitude, extending the picture of fundamental physics down to scales 5×10^{-20} m with the help of the high-energy processes at the Large Hadron Collider (LHC).

[1] A very interesting book by Paul de Kruif, published 100 years ago, another anniversary, reports on this progress.

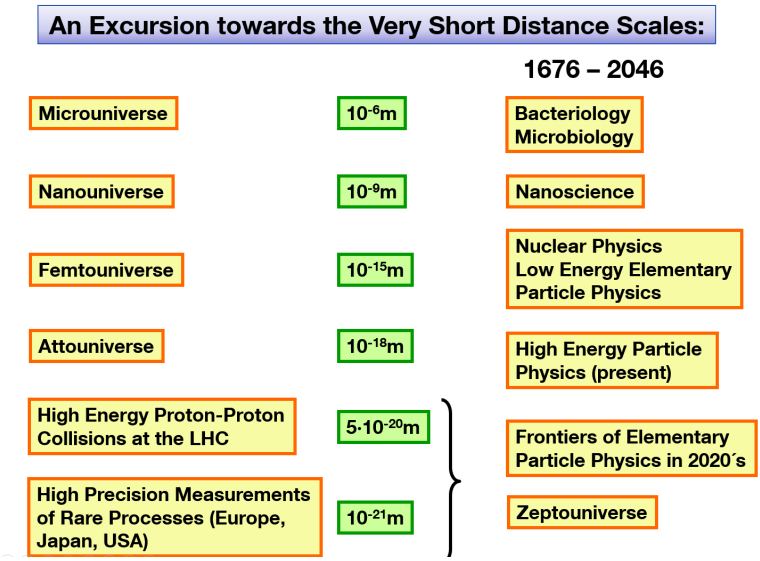

Fig. 2. Progress in resolving short-distance scales 1676–2026.

Further resolution, down to scales as short as 10^{-21} m (*Zeptouniverse*) or even shorter scales, should be possible with the help of high-precision experiments in which flavour-violating processes played a prominent role for decades. This is evident from my recent *Flavour Autobiography* [1].

Let us recall the particles of the Standard Model that have all been discovered. They are collected in Fig. 3. The small red stars indicate which particles were known in 1970 when I was doing my Master's thesis. The big red star is reserved for the Higgs. Certainly, a dramatic progress has been made since 1970.

My *Flavour Autobiography* is 323 pages long and I thought that it could turn out to be useful to extract from it the most important strategies for the search for New Physics (NP). This is the main topic of this write-up. I arranged the material as follows.

In Section 2, I will list the main reasons why we are sure that NP beyond the SM must exist. In Section 3, I will present the *Dual Picture of Short Distance Scales* that I have been presenting in numerous talks since 2009 but not in print except for [1] recently. It demonstrates in an impressive manner that the scales explored in particle physics are indeed very short. In Section 4, I will present an express summary of the basic framework in weak decays. To this end, I will use two colourful figures from my talks. Having this, I will list prerequisites for a successful search for NP and summarize their present status.

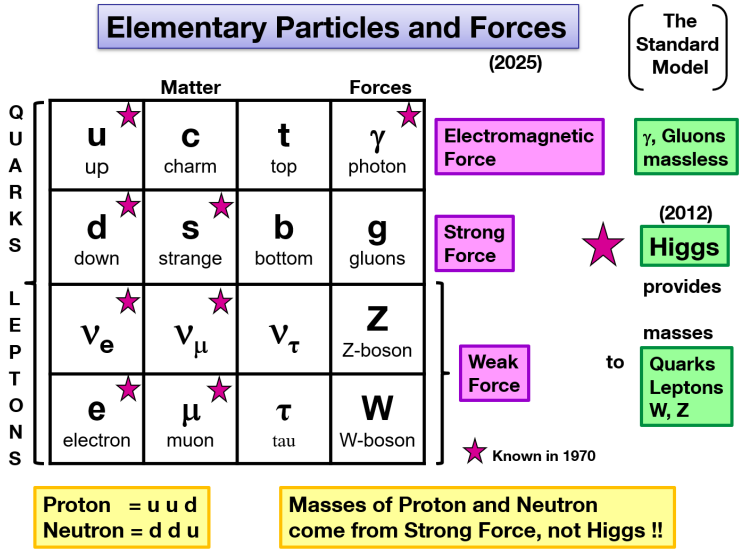

Fig. 3. The particles of the Standard Model.

Next, in Section 5, I will describe very briefly the structure of the Weak Effective Theory (WET) and the Standard Model Effective Field Theory (SMEFT). Beginning with phenomenology in the SM, I will describe in Section 6 the main ideas behind the strategy developed with Elena Venturini that avoids present inconsistencies in the determination of the CKM element $|V_{cb}|$ that plays a very important role in FCNC processes. Subsequently, in Section 7, I will illustrate with colourful plots the so-called *DNA-Strategy* developed this time with Jennifer Girrbach-Noe.

Next, in Section 8, a short description of the most popular New Physics models will be given. They can be distinguished through correlations between various observables. We demonstrate this in Section 9 which can be considered as an album of correlations. It will consist of several plots showing correlations in various NP models. In Section 10, we present the status of the analyses of correlations between observables within the SMEFT. Finally, in Section 11, the summary and an outlook on the coming years will be given.

2. Basic questions beyond the Standard Model

The Standard Model (SM) describes the data very well, but there are a number of fundamental questions that it cannot answer. They are well known, but let us list them again.

The nature of dark matter: What is the particle nature of dark matter, which makes up about 27% of the matter in the Universe but is absent from the SM?

Dark energy and the accelerated expansion of the Universe: What is responsible for the observed accelerated expansion of the Universe?

Neutrino masses: Why do neutrinos have tiny but non-zero masses, whereas they are massless in the SM? Are neutrinos Dirac fermions like in the SM or maybe Majorana fermions, *i.e.* their own antiparticles? This would indicate that lepton number is not a fundamental symmetry of nature. Neutrinoless double-beta decay would establish this property. Do right-handed neutrinos exist?

Matter–antimatter asymmetry: Why is the Universe dominated by matter rather than antimatter? This is related to the violation of CP-symmetry soon after the Big Bang and is crucial for our existence. The size of CP violation in the SM is by far insufficient to explain this.

The hierarchy problem: Why is the Higgs boson mass so much lighter than the Planck scale? Is it a fundamental particle or a composite particle arising from some new strong dynamics responsible for the spontaneous breakdown of the electroweak symmetry of the SM? Is the form of the Higgs potential affected by NP?

The origin of flavour: What determines the pattern of fermion masses and mixing angles? Why is the top-quark mass larger by five orders of magnitude than the electron mass and eleven orders of magnitude larger than neutrino masses? What is the origin of the pattern of quark and lepton interactions summarized by the CKM and PMNS matrices?

The strong CP problem: Why is CP violation in strong interactions so small? Will axions arising from related solutions be discovered in the near future?

Unification of forces: Do the fundamental forces unify at high energies? Numerous ideas have been presented in the last fifty years.

Is supersymmetry realized in nature? While, until the discovery of the Higgs, supersymmetric extensions of the SM were leading our field, it does not appear to be the case now. But supersymmetry could still be realized at much higher energy scales.

Quantum gravity: How can gravity be consistently combined with quantum field theory?

Number of generations: Why are there exactly three generations of quarks and leptons? While the existence of a fourth generation of chiral fermions has by now been excluded, several generations of vector-like quarks and leptons remain possible.

CP violation in the lepton sector? If established, it would strengthen the case of leptogenesis related to the dominance of matter in the Universe.

In view of these questions, it is obvious that new forces and new particles beyond those shown in Fig. 3 must exist and our duty is to find them somehow. As far as flavour physics is concerned, the basic questions are listed in more detail in Fig. 4.

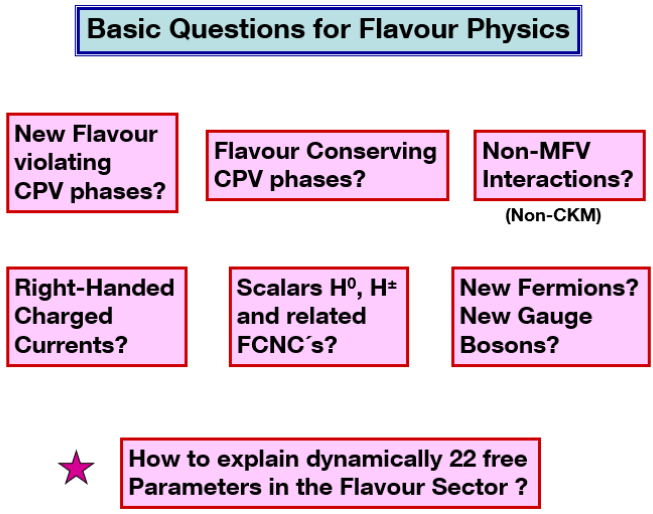

Fig. 4. Basic questions for flavour physics.

3. Dual picture of short-distance scales

Our colleagues in Astrophysics and Cosmology can easily impress the community by showing impressive pictures of the Universe at large. One can look at them with naked eyes or powerful telescopes. This is much harder in particle physics, as with good eyes, one can sense 10^{-4} m, and using microscopes that are more powerful, one can see the picture of the nanouniverse but not really of short-distance scales explored in particle physics.

While preparing my talk at the EPS-2009 in Cracow [2], I got the idea to improve this situation by simply removing the minus sign from the exponential, that is instead of using 10^{-x} m, I proposed to use 10^{x} m. After all, what matters is the relative size to our hight which for adults is roughly 1.75 ± 0.20 m.

In fact, in this manner, one can really get impressed by the shortness of the scales resolved in particle physics. In Figs. 5 and 6, I show the dual pictures of the following Universes:

Dual picture of the microuniverse

This corresponds to the distance from Munich to Copenhagen, where in 1972 I completed my Ph.D. studies. See the left picture in Fig. 5.

Dual picture of the nanouniverse

Looking at the moon, one can get impressed by the distance scales explored by the nanotechnologists. See the right picture in Fig. 5. Indeed,

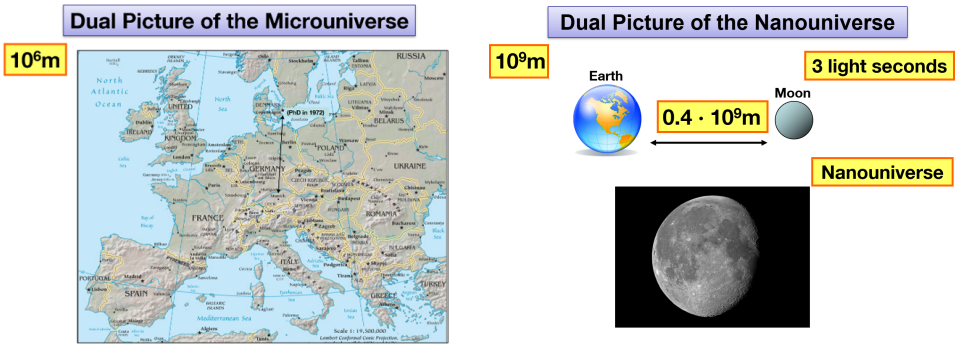

Fig. 5. Dual Picture of the Microuniverse (left) and of the Nanouniverse (right).

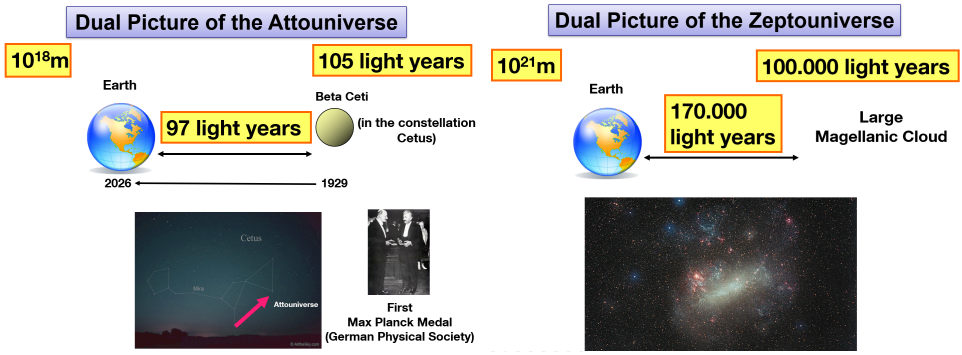

Fig. 6. Dual picture of the attouniverse (left) and of the zeptouniverse (right). (Wikipedia)

if we were as tall as the distance from the Earth to the Moon, they would explore the distance scales of a few meters. At first sight, very impressive but cannot really compete with what particle physicists can achieve.

Dual picture of the attouniverse

Indeed, already the Attouniverse is much more impressive than the nanouniverse. Let us assume that, during the celebration of the first Max Planck Medal (1929), given to Albert Einstein and Max Planck himself, a signal has been sent from Beta Ceti (an object in the constellation Cetus, at a distance of roughly 10^{18} m from us, see Fig. 6 (left)) to the Earth. It will arrive only this year.

Dual picture of the zeptouniverse

We make the next step to the Large Magellanic Cloud, see Fig. 6 (right). Let us then assume that a signal from there will arrive on the Earth this

year. One can then ask what was on the Earth when this signal was sent to us. Certainly there was no LHCb, CDF, ATLAS or Belle II collaborations but another one with different goals as seen on the left in Fig. 7. The first guy on the left was probably the spokesman of this collaboration. I doubt he expected to be cited by anybody in 2026.

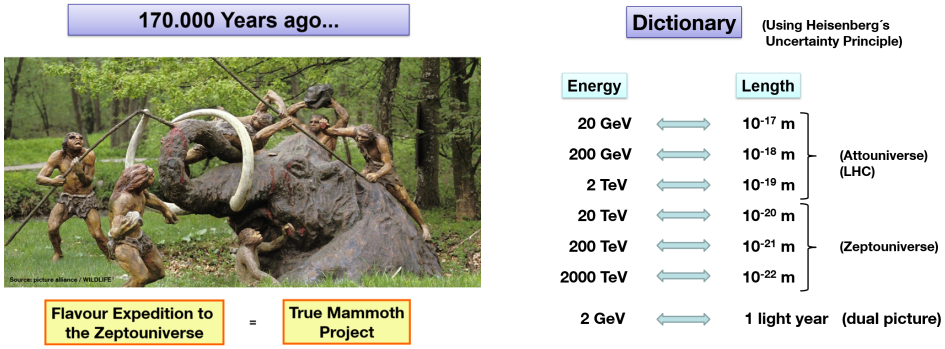

Fig. 7. Old collaboration at work (left) and the dictionary (right).

As is evident from my recent *Flavour Autobiography* [1], this picture fits very well to the efforts of many flavour physicists: *Flavour Expedition* to very short distance scales with the goal to discover new animalcula. It is indeed the true Mammoth Project. This will also be evident as we continue.

The dictionary between energy scales explored by present and future colliders and distance scales used to construct this dual picture of short distances is shown on the right in Fig. 7.

4. Basic framework and prerequisits for finding NP

In Fig. 8, I show the basis of effective theories which is the operator product expansion, the sum of operators multiplied by the Wilson Coefficients [3–5]. In Fig. 9, the master formula for weak-decay amplitudes is shown and different contributions are briefly explained. Detailed explanations can be found in my book [6] and in other reviews, in particular in my Les Houches lectures [7]. The typical Feynman diagrams in flavour physics of the SM are penguin and box diagrams. They are shown in Fig. 10.

This information should be sufficient for this lecture but the following paragraphs should bring additional insight into these matters.

Let me stress first that in the indirect search for NP with the help of weak decays, particle–antiparticle mixing observables, Electric Dipole Moments (EDMs), and other observables, the first very important step is to obtain SM predictions as accurate as possible. Simply because the first hints for NP in an indirect search will come from deviations from SM expectations.

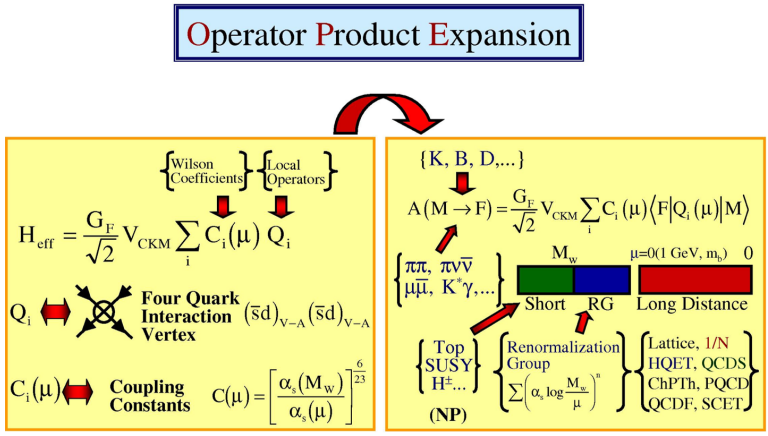

$$\left\langle \overline{K}^0 \left| (\bar{s}d)_{V-A} (\bar{s}d)_{V-A} \right| K^0 \right\rangle = \frac{8}{3} \hat{B}_K \, F_K^2 \, m_K^2 \left[\alpha_s(\mu) \right]^{2/9}$$

Fig. 8. Operator product expansion.

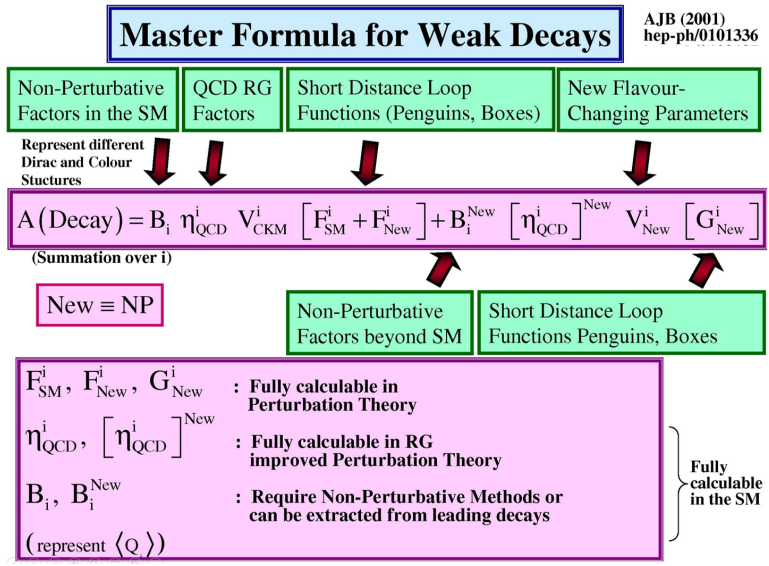

Fig. 9. Master formula for weak-decay amplitudes.

As the masses of the involved SM quarks and leptons, gauge bosons and the Higgs are by now very well known and this also applies to gauge couplings, the main challenge in obtaining precise SM predictions for the processes in question are:

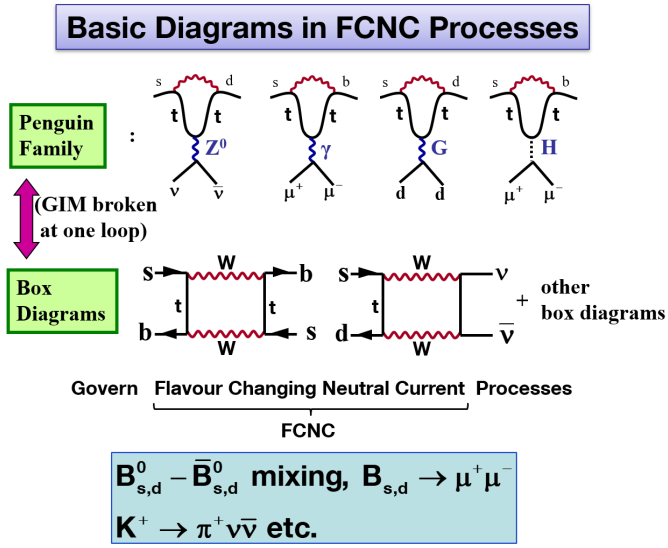

Fig. 10. Basic diagrams in FCNC processes in the Standard Model.

— Calculations of short-distance QCD, QED, and electroweak corrections. These are the loop functions $F^i_{\rm SM}$ and factors $\eta^i_{\rm QCD}$ in Fig. 9.

— Calculations of non-perturbative QCD effects. They are represented by the factors B_i in Fig. 9.

— Determination of CKM and PMNS parameters.

— Precise experimental measurements of the observables involved.

In my view, the first challenge on this list has been overcome to a large extent as described in Part V of [1] and in [8]. Impressive progress has also been made by Lattice QCD (LQCD) in the evaluation of non-perturbative QCD effects with regular reports from FLAG [9]. This is in particular the case for particle–antiparticle mixing, weak-decay constants, form factors, *etc.* Similar ChPT made important contributions here [10]. In this manner, leptonic meson decays contain by now only small non-perturbative uncertainties. This is also the case for semileptonic FCNCs with neutrinos in the final state, where the main challenge are form factors. Significant progress on them has been made in the last ten years [11–14].

The case of semileptonic decays with charged leptons in the final state is another story due to non-factorizable long-distance contributions that require detailed studies. Presently, they do not allow for a unique agreement between various theoretical groups on whether the anomalies observed in

$b \to s\ell^+\ell^-$ transitions result from NP or non-perturbative effects. There is a very rich literature on this subject and I list here only few papers in which further references can be found [15–22].

Unfortunately, the situation is even worse in the case of non-leptonic meson decays where the non-perturbative uncertainties remain large. See Parts III and XI in [1] for the most recent summary of the present status.

Another issue are CKM parameters that are free parameters in the SM and have to be determined from experiment, preferably from tree-level decays that are believed to be less affected by NP than loop-induced processes like FCNC processes within the SM. Unfortunately, there are inconsistencies between different determinations of some CKM parameters, in particular $|V_{cb}|$. This introduces significant uncertainties in decays such as $K^+ \to \pi^+\nu\bar{\nu}$ and $K_{\rm L} \to \pi^0\nu\bar{\nu}$ that are sensitive functions of $|V_{cb}|$. I will return to this issue in Section 6.

Finally, crucial are the measurements of various observables, such as weak-decay branching ratios, CP asymmetries, mass differences $\Delta M_{s,d}$, *etc.* Some are already measured with respectable precision, others should be measured in the coming years but for several we will have to wait still for a decade or more. The related branching ratios are simply tiny.

5. SMEFT and WET

These days, two general effective theories play an important role in particle physics: SMEFT and WET. I want to describe briefly what they are. In this context, Fig. 11 is very useful. It deals with the so-called *Top-Down Approach*.

5.1. SMEFT

Let us assume we constructed a new model, the UV completion of the SM, which is supposed to answer some of the questions listed above and to describe the anomalies (departures from SM predictions) observed in experiments. It is an extension of the SM that contains new particles and new forces. The latter are described by new gauge symmetries that are spontaneously broken directly or in steps down to the SM gauge group at some scale Λ at which the lightest new particles have been integrated out. Below Λ, only SM particles appear and the gauge symmetry is the unbroken gauge group of the SM

$$\mathrm{SU}(3)_C \otimes \mathrm{SU}(2)_{\rm L} \otimes \mathrm{U}(1)_Y\,, \tag{1}$$

provided Λ is significantly larger than the electroweak (EW) scale $\mu_{\rm ew}$.

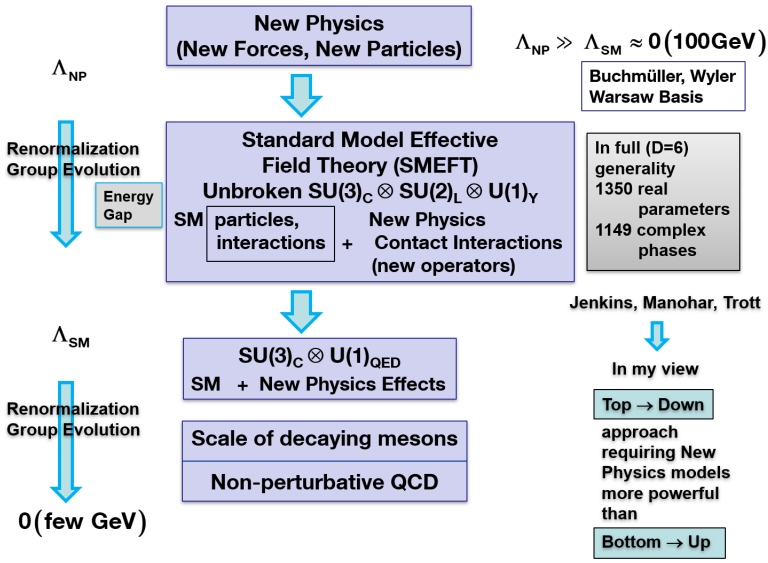

Fig. 11. Grand view of the RG evolution in the SMEFT.

The Effective Field Theory (EFT) with the unbroken SM gauge group is usually called the Standard Model Effective Field Theory (SMEFT) [23, 24] because at low energies, it should reduce to the SM, provided no undiscovered weakly coupled *light* particles exist, such as axions or sterile neutrinos. For recent reviews on the SMEFT, see [25–27].

However, the presence of new operators, in particular dimension six ones, whose Wilson coefficients (WCs) can be calculated in a given model as functions of its parameters, can introduce very significant modifications of SM predictions for flavour observables. Also the values of SM parameters can be modified in this manner. This is also the case for the WCs of the involved operators which are generated in the SM and, being modified, contain information about NP beyond the SM. Moreover, there is a multitude of operators that are strongly suppressed in the SM but can be important in the SMEFT. Therefore, the name SMEFT is to some extent a misnomer but as the basic gauge symmetry is the SM one, it has been accepted by the particle physics community.

The structure of the interactions in the SMEFT, even if governed by the SM gauge group, depends on the UV completion considered. This is important because otherwise there would be no chance to find out anything about the dynamics above the scale Λ. In particular, the number of free parameters will depend on the fundamental theory or model considered. These parameters can be conveniently defined at the scale Λ. Their number depends on the theory considered and it will not change when the renormal-

ization group (RG) evolution down to the electroweak scale is performed. Only their values will change as well as the values of the WCs in the effective theory describing the physics between the scale Λ and the electroweak scale.

This physics, beyond that one of the SM, is described by an effective Lagrangian

$$\mathcal{L}^{(6)} = \sum_k C_k^{(6)} Q_k^{(6)} \,, \tag{2}$$

where, for simplicity, we keep only the contributions of dimension six. Other contributions are discussed in detail in numerous papers [25–27] and the ones listed below.

The number of operators and their Dirac structure depend generally on the model considered. However, to be prepared for all possible models and to develop a general framework, one can classify operators in full generality by imposing only the SM gauge symmetry in (1). This has been done in [23, 24]. The second of these papers removed certain redundant operators present in the first one and these days the results of [24] are used. However, by no means should the pioneering work of Buchmüler and Wyler be underestimated. The corresponding RG analysis at leading order (LO) of all these operators has been presented in [28–30].

It turns out that for three generations of fermions, there are 2499 independent operators $Q_k^{(6)}$ (59 irreducible flavour representations) that do not violate baryon and lepton number. This means that the RG analysis involves, in full generality, a 2499×2499 anomalous dimension matrix[2] with the evolution governed by the Higgs self-coupling λ [28], the Yukawa couplings [29], and the SM gauge interactions [30]. The status of the calculations of anomalous dimensions at the leading and next-leading order is summarized in [1, 27] with the second paper presenting technical details.

5.2. WET

The SMEFT Renormalization Group Equations (RGEs) allow for calculating the WCs of the SMEFT at the electroweak scale. Below the electroweak scale, the interactions are governed not by the full gauge symmetry of the SM but by

$$\mathrm{SU}(3)_C \otimes \mathrm{U}(1)_{\mathrm{QED}} \,, \tag{3}$$

which is very familiar to us. However, in the presence of NP, there are new operators generated already at the NP scale and/or at the electroweak scale through RG running in the SMEFT and through the matching onto the low-energy theory described by this reduced symmetry. Consequently, the starting point for the RG evolution from the electroweak scale down

[2] Fortunately, as seen in Fig. 1 of [27], there are very many vanishing elements in this matrix.

to the low-energy scale differs from the one encountered within the SM. Not only the initial conditions for SM WCs at the electroweak scale can be modified by NP but new WCs might also be present. The resulting effective theory below the electroweak scale, although as the SM based on the gauge symmetry of QCD×QED, differs then from the SM and is called the Weak Effective Theory (WET). It should be stressed that this theory does not involve W, Z gauge bosons, the Higgs boson, and the top quark as dynamical degrees of freedom. Moreover, there are no elementary scalars in this theory.

The counting of all possible gauge-invariant operators of the WET has been accomplished in [31]. There are 70 hermitian $D = 5$ and 3631 hermitian $D = 6$ operators that conserve baryon and lepton numbers, as well as $\Delta B = \pm\Delta L = \pm 1$, $\Delta L = \pm 2$, and $\Delta L = \pm 4$ operators. Among the 3631 operators in question, 1933 are CP-even and 1698 CP-odd.

This counting shows clearly that in order for a model to be predictive, the number of free parameters has to be reduced by much. In particular, flavour symmetries play an important role here. The reviews in [26, 27] describe them in some detail and contain several references to original papers in which these flavour symmetries have been proposed and investigated phenomenologically.

It is now evident that searching for NP indirectly is a true Mammoth Project. This becomes even clearer by reading Part II of [27] which makes the anatomy of operator mixing in the process of the renormalization group evolution from Λ down to $\mu_{\rm ew}$. But we should not give up because NP could be as beautiful as the photo in Fig. 12 which has been taken by our younger son Allan during his expedition related to climate rather than flavour.

This photo actually describes the so-called Bottom-Up Approach. In this approach, one first tries to describe various departures of the low-energy data from SM expectations by modifying the WCs of SM operators and/or adding new operators. Sometimes only a small number of new operators and related WCs is sufficient to describe the data. Having their values at the electroweak scale, one can then, as a first step, construct simplified NP models which could imply the presence of these new operators and the modifications of SM WCs. Subsequently, one can try to develop a more sophisticated model, like in the top-down approach. from which these WCs would result.

Thus, in practice, one tries to borrow the lessons from both approaches because, while by definition, in the top-down approach, one knows better the fundamental new theory at short-distance scales, in the bottom-up approach, one has close contact with the data which the fundamental theory is supposed to describe.

But the route can be very tough as summarized in Fig. 12 with the crevasses representing difficult theoretical calculations and difficult experimental measurements.

Let us then move to a strategy which allows efficiently to identify anomalies in experimental data giving signs of the NP at work.

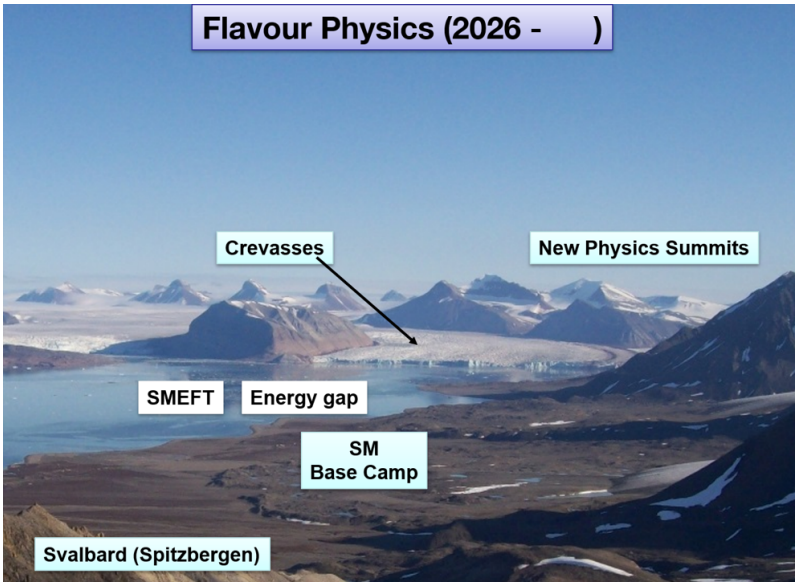

Fig. 12. SMEFT and New Physics summits.

6. Removing $|V_{cb}|$ uncertainties

As already stressed above, in order to identify the presence of NP, high precision of SM prediction is crucial. This is the main goal of the strategy described now. In order to motivate this strategy in explicit terms, let us recall the values of $|V_{cb}|$ extracted from inclusive and exclusive tree-level semi-leptonic $b \to c$ decays [9, 32]

$$|V_{cb}|_{\rm incl} = (41.97 \pm 0.48) \times 10^{-3}\,, \qquad |V_{cb}|_{\rm excl} = (39.21 \pm 0.62) \times 10^{-3}\,. \quad (4)$$

Since rare K and B decays and mixing parameters are sensitive functions of $|V_{cb}|$, varying it from 39×10^{-3} to 43×10^{-3} changes $\Delta M_{s,d}$ and B-decay branching ratios by roughly 21%, $K^+ \to \pi^+ \nu\bar{\nu}$ branching ratio by 31%, ε_K by 39%, and $K_{\rm L} \to \pi^0 \nu\bar{\nu}$ and $K_{\rm S} \to \mu^+\mu^-$ branching ratios by 48%.

Based on my report in Part V in [1], these uncertainties are clearly a disaster for those like me, my collaborators, and other experts in NLO and NNLO calculations who spent decades to reduce theoretical uncertainties in basically all important rare K and B decays and quark mixing observables down to (1–2)%.

It is also a disaster for lattice QCD experts who, for quark mixing observables and in particular meson weak-decay constants, achieved the accuracy at the level of a few percent. Also, significant progress on form factors from LQCD and Light-Cone Sum Rules has been done.

In order to motivate this strategy further, I show in Fig. 13 the dependence of $K^+ \to \pi^+\nu\bar{\nu}$ and $K_{\rm L} \to \pi^0\nu\bar{\nu}$ branching ratios on $|V_{cb}|$, β, and γ with β and γ being the angles of the Unitarity Triangle shown in Fig. 14. This dependence has already been studied with Monika Blanke in [33] but this particular figure is from the first paper with Elena Venturini with few details described soon [34].

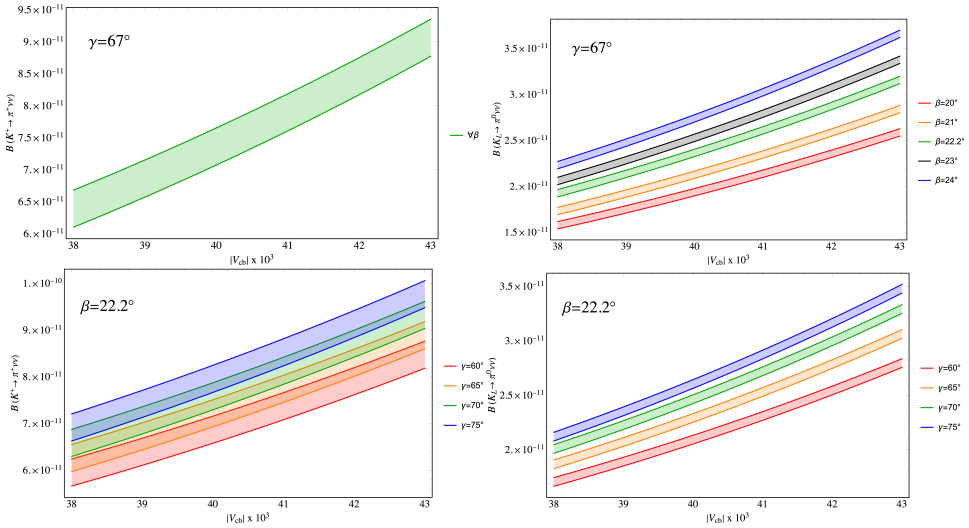

Fig. 13. The dependence of the branching ratios $\mathcal{B}(K^+ \to \pi^+\nu\bar{\nu})$ (left panels) and $\mathcal{B}(K_{\rm L} \to \pi^0\nu\bar{\nu})$ (right panels) on $|V_{cb}|$ for different values of $\beta = 20.0°, 21.0°, 22.0°, 23.0°, 24.0°$ at fixed $\gamma = 67°$, and for different values of $\gamma = 60.0°, 65.0°, 70.0°, 75°$ at fixed $\beta = 22.2°$. The width of the bands represents the uncertainties whose origin is not related to the γ, β, and $|V_{cb}|$ parameters. From [34].

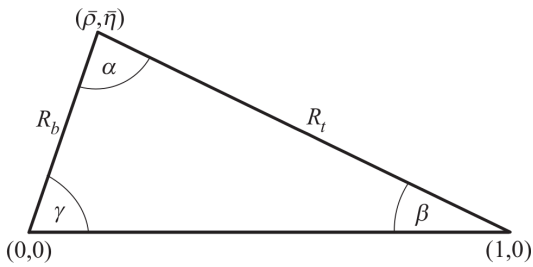

Fig. 14. The Unitarity Triangle.

One observes that the largest uncertainties on these branching ratios are due to the $|V_{cb}|$ parameter: the elimination of this source of error is the main focus of [34]. This idea was already born in 2003 in the context of $B_{s,d} \to \mu\bar{\mu}$ and $\Delta M_{s,d}$ [35]. Just considering the ratio of these two observables allowed to eliminate the dependence on the CKM parameters, in particular $|V_{cb}|$ and the weak-decay constants F_{B_q}, poorly known in 2003, leaving the main uncertainty in the non-perturbative parameters $\hat{B}_q$ entering ΔM_q. In 2026, these parameters are known from LQCD with respectable precision. We show some of them in Table 1.

Table 1. Selected input values used in $\Delta F = 2$ and other flavour-changing processes. For future updates, see FLAG [40], PDG [36], and HFLAV [37].

m_{B_s}	$=$	$5366.8(2)\,\text{MeV}$ [36]	m_{B_d}	$=$	$5279.58(17)\,\text{MeV}$ [36]
ΔM_s	$=$	$17.749(20)\,\text{ps}^{-1}$ [36]	ΔM_d	$=$	$0.5065(19)\,\text{ps}^{-1}$ [36]
β	$=$	$22.62(45)^\circ$ [37]	F_K	$=$	$155.7(3)\,\text{MeV}$ [38]
$\hat{B}_K$	$=$	$0.7627(60)$ [39]	$\lvert\epsilon_K\rvert$	$=$	$2.228(11) \times 10^{-3}$ [36]
F_{B_s}	$=$	$230.3(1.3)\,\text{MeV}$ [40]	F_{B_d}	$=$	$190.0(1.3)\,\text{MeV}$ [40]
$F_{B_s}\sqrt{\hat{B}_s}$	$=$	$256.1(5.7)\,\text{MeV}$ [41]	$F_{B_d}\sqrt{\hat{B}_d}$	$=$	$210.6(5.5)\,\text{MeV}$ [41]
$\hat{B}_s$	$=$	$1.232(53)$ [41]	$\hat{B}_d$	$=$	$1.222(61)$ [41]
τ_{B_s}	$=$	$1.515(4)\,\text{ps}$ [42]	τ_{B_d}	$=$	$1.519(4)\,\text{ps}$ [42]

In the spring of 2021, in a paper with Christoph Bobeth, an update of my 2003 paper, the search for NP with the help of this ratio has been reemphasized [43]. Finally, using the 2+1+1 flavour results of [41], Elena Venturini and I found [44]

$$R_{s\mu} = \frac{\bar{\mathcal{B}}\,(B_s \to \mu^+\mu^-)}{\Delta M_s} = \left(2.130^{+0.083}_{-0.053}\right) \times 10^{-10}\ \text{ps}\,, \tag{5}$$

$$R_{d\mu} = \frac{\mathcal{B}\,(B_d \to \mu^+\mu^-)}{\Delta M_d} = \left(2.005^{+0.089}_{-0.066}\right) \times 10^{-10}\ \text{ps}\,. \tag{6}$$

Consequently, in the SM, the predictions for $B_q \to \mu\bar{\mu}$ branching ratios are rather precise as ΔM_q have already been precisely measured. Their values, together with the present experimental values, are given in Table 2.

In the fall of 2021, my strategy of 2003 has been generalized in collaboration with Elena to semi-leptonic B and K decays [34]. We have constructed a number of $|V_{cb}|$-independent ratios. Let me just list the most interesting ones. Others can be found in the latter paper as well as in [44–46] and [1].

Table 2. Present the most accurate SM estimates of the branching ratios obtained using the BV-strategy. These are *the Magnificent Seven* decays, that being theoretically the cleanest are optimal for the search for NP. Few numbers differ from the similar table in [46] due to the modification of β and the NNLO QCD corrections to $X(x_t)$ (Talk of Emanuel Stamou at the international conference Kaon 25).

Decay	SM Branching ratio	Data	
$B_s \to \mu^+\mu^-$	$\left(3.78^{+0.15}_{-0.10}\right) \times 10^{-9}$	$(3.45 \pm 0.29) \times 10^{-9}$	[50]
$B_d \to \mu^+\mu^-$	$\left(1.02^{+0.05}_{-0.03}\right) \times 10^{-10}$	$\leq 2.05 \times 10^{-10}$	[51]
$B^+ \to K^+\nu\bar{\nu}$	$(4.99 \pm 0.30) \times 10^{-6}$	$(13 \pm 4) \times 10^{-6}$	[52]
$B^0 \to K^{0*}\nu\bar{\nu}$	$(10.25 \pm 0.92) \times 10^{-6}$	$\leq 1.5 \times 10^{-5}$	[53]
$K^+ \to \pi^+\nu\bar{\nu}$	$(8.65 \pm 0.42) \times 10^{-11}$	$\left(9.6^{+1.9}_{-1.8}\right) \times 10^{-11}$	(NA62)
$K_{\rm L} \to \pi^0\nu\bar{\nu}$	$(3.05 \pm 0.17) \times 10^{-11}$	$\leq 2.0 \times 10^{-9}$	[54]
$(K_{\rm S} \to \mu\bar{\mu})_{\rm SD}$	$(1.85 \pm 0.12) \times 10^{-13}$	$\leq 2.1 \times 10^{-10}$	[55]

In particular, one has not included NNLO corrections to $X(x_t)$

$$\frac{\mathcal{B}\left(K^+ \to \pi^+\nu\bar{\nu}\right)}{|\varepsilon_K|^{0.82}} = (1.27 \pm 0.06) \times 10^{-8} \left(\frac{\sin\gamma}{\sin 64.6^\circ}\right)^{0.015} \left(\frac{\sin 22.6^\circ}{\sin\beta}\right)^{0.71}, \tag{7}$$

$$\frac{\mathcal{B}\left(K_{\rm L} \to \pi^0\nu\bar{\nu}\right)}{|\varepsilon_K|^{1.18}} = (4.03 \pm 0.21) \times 10^{-8} \left(\frac{\sin\gamma}{\sin 64.6^\circ}\right)^{0.03} \left(\frac{\sin\beta}{\sin 22.6^\circ}\right)^{0.98}. \tag{8}$$

Moreover, one finds

$$\frac{\mathcal{B}\left(K^+ \to \pi^+\nu\bar{\nu}\right)}{\left[\bar{\mathcal{B}}\left(B_s \to \mu^+\mu^-\right)\right]^{1.4}} = 53.46 \pm 2.75\,, \tag{9}$$

$$\frac{\mathcal{B}\left(K^+ \to \pi^+\nu\bar{\nu}\right)}{\left[\mathcal{B}\left(B^+ \to K^+\nu\bar{\nu}\right)\right]^{1.4}} = (2.28 \pm 0.13) \times 10^{-3}\,, \tag{10}$$

$$\frac{\mathcal{B}\left(B^+ \to K^+\nu\bar{\nu}\right)}{\bar{\mathcal{B}}\left(B_s \to \mu^+\mu^-\right)} = (1.32 \pm 0.07) \times 10^{3}\,. \tag{11}$$

As within the SM, the values of ΔM_d, ΔM_s, and ε_K are just equal to their well-measured experimental values, it is possible to determine several of the branching ratios with best precision to date. We list them in Table 2.

Moreover, it is possible to determine all CKM parameters

$$\begin{aligned} |V_{cb}| &= 42.5(5) \times 10^{-3}\,, \qquad \gamma = 64.6(16)^\circ\,, \\ \beta &= 22.62(45)^\circ\,, \qquad |V_{ub}| = 3.76(11) \times 10^{-3}\,, \end{aligned} \tag{12}$$

and consequently,

$$|V_{ts}| = 41.8(4) \times 10^{-3}\,, \quad |V_{td}| = 8.64(14) \times 10^{-3}\,, \quad \mathrm{Im}\lambda_t = 1.45(5) \times 10^{-4}\,, \tag{13}$$

$$\bar{\varrho} = 0.165(12), \qquad \bar{\eta} = 0.348(11)\,, \tag{14}$$

where $\lambda_t = V_{ts}^* V_{td}$.

Let me next stress that presently, the optimal set of CKM variables is the following one [33]:

$$|V_{us}|\,, \qquad |V_{cb}|\,, \qquad \beta\,, \qquad \gamma\,, \tag{15}$$

which avoids the use of $|V_{ub}|$ as a fundamental parameter. In this context, let me present two simple formulae that allow one, having (β, γ), to calculate the apex of the UT in no time, but to my knowledge they have been presented only recently for the first time [47, 48]. They read

$$\bar{\varrho} = \frac{\sin\beta\cos\gamma}{\sin(\beta+\gamma)}, \qquad \bar{\eta} = \frac{\sin\beta\sin\gamma}{\sin(\beta+\gamma)}\,. \tag{16}$$

Evidently, they can be derived by high-school students, but the UT is unknown to them and somehow, no flavour physicist got the idea to present them in print so far. Numerical tables for $\bar{\varrho}$ and $\bar{\eta}$ for different values of β and γ are given in [47, 48].

Next, taking the present experimental result for $B_s \to \mu^+\mu^-$ allows one to determine the present $|V_{cb}|$-independent experimental values for the ratios in (9) and (11) that read

$$\frac{\mathcal{B}\,(K^+ \to \pi^+\nu\bar{\nu})_{\rm exp}}{\left[\bar{\mathcal{B}}\,(B_s \to \mu^+\mu^-)\right]^{1.4}_{\rm exp}} = 67.52 \pm 15.09\,, \qquad \mathrm{SM} : 53.46 \pm 2.75\,, \tag{17}$$

$$\frac{\mathcal{B}\,(B^+ \to K^+\nu\bar{\nu})_{\rm exp}}{\bar{\mathcal{B}}\,(B_s \to \mu^+\mu^-)_{\rm exp}} = (3.8 \pm 1.2) \times 10^3\,, \qquad \mathrm{SM} : (1.32 \pm 0.07) \times 10^3\,. \tag{18}$$

The first ratio is consistent with the SM but the second one differs significantly from the very precise SM value. Let us hope that the experimental errors on these ratios will decrease in the coming years and the data will depart more from the SM predictions. I wish Belle II, NA62, LHCb, CMS, and ATLAS experimentalists luck in measuring precisely the involved branching ratios.

Since the results presented in Table 2 and the ones for CKM parameters above assume no NP in $\Delta F = 2$ observables, a useful rapid test of this assumption is provided by the following, practically CKM-free, SM relation between the four $\Delta F = 2$ observables [45]:

$$\frac{|\varepsilon_K|^{1.18}}{\Delta M_d\,\Delta M_s} = (8.37 \pm 0.18) \times 10^{-5} \left(\frac{\sin\beta}{\sin 22.62^\circ}\right)^{1.027} K\,\mathrm{ps}^2\,, \tag{19}$$

where

$$K = \left(\frac{\hat{B}_K}{0.7625}\right)^{1.18} \left[\frac{210.6\,\mathrm{MeV}}{\sqrt{\hat{B}_{B_d}}F_{B_d}}\right]^2 \left[\frac{256.1\,\mathrm{MeV}}{\sqrt{\hat{B}_{B_s}}F_{B_s}}\right]^2 = 1.00 \pm 0.07\,. \tag{20}$$

The dependence on $|V_{cb}|$ drops out and the one on γ being negligible is included in the uncertainty varying γ in the range $60^\circ \le \gamma \le 70^\circ$. Inserting the experimental values of the three $\Delta F = 2$ observables on the LHS one finds for this ratio $(8.26 \pm 0.06) \times 10^{-5}$. Consequently, with the presently known values of $\sqrt{\hat{B}_{B_d}}F_{B_d}$ and $\sqrt{\hat{B}_{B_s}}F_{B_s}$ from HPQCD, $\hat{B}_K$ from RBC-UKQCD, and the present value of β from $S_{\psi K_S}$, the SM is performing in the $\Delta F = 2$ sector indeed very well. However, with the $2+1$ flavours from Fermilab Lattice and MILC collaborations (FNAL/MILC) [49], the central value on the RHS of (19) decreases to $(6.29 \pm 0.18) \times 10^{-5}$, so that the fact that this ratio agrees with the data for present values of hadronic parameters with $2+1+1$ flavours and the experimental value of β is remarkable. Therefore, it is very important that a second lattice collaboration performs the calculation of $\sqrt{\hat{B}_{B_d}}F_{B_d}$ and $\sqrt{\hat{B}_{B_s}}F_{B_s}$ with $2+1+1$ flavours.

7. DNA strategy

The strategy just presented allows us to identify quickly the ratios of observables affected by NP. In order to find out what this NP could be, we have to do more.

In my view, the fastest route to select the candidates for NP models before doing global fits is the strategy developed in collaboration with Jennifer Girrbach-Noe [56]. The main idea is to study first the patterns of anomalies observed in the data and compare them with the patterns of deviation from SM predictions in a given NP scenario. Such patterns, that expose suppressions and enhancements of various observables relative to SM predictions, can be considered as DNAs of the animalcula hunted by us. In particular, the correlations between various enhancements and suppressions can rule out some NP scenarios already before any global fit is performed.

This strategy, proposed by us in 2013 [56], has been documented in several subsequent papers, in particular in Chapter 19.4 of my book [6] and recently in [1, 57] with many colourful plots. Still, I want to summarize its main steps and show some of these plots.

Step 1

We construct a chart showing different observables, typically a branching ratio for a given decay or an asymmetry, such as CP-asymmetries $S_{\psi K_S}$ and $S_{\psi\phi}$, and quantities ΔM_s, ΔM_d, ε_K, and ε'/ε. The important point is to select the optimal set of observables which are simple enough so that definite predictions in a given theory can be made and can be measured in the coming decades. The ones in Table 2 are examples of such observables among the rare K and B decays.

Step 2

In a given NP model, we calculate the selected observables and investigate whether a given observable is *enhanced or suppressed* relative to the SM prediction or is basically unchanged. What this means requires a measure, like three σ. For these three situations, one can use the following colour coding:

enhancement no change **suppression**. (21)

To this end, the predictions within the SM have to be known precisely.

Step 3

It is only seldom that a given observable in a given theory is uniquely suppressed or enhanced but frequently two observables are correlated or uncorrelated with each other. That is, the enhancement of one observable implies uniquely an enhancement (correlation) or suppression (anti-correlation) of another observable. It can also happen that no change in the value of a given observable implies no change in another observable. This is illustrated in Fig. 15.

The idea then is to connect in our DNA chart a given pair of observables that are correlated with each other by a line. Absence of a line means that two given observables are uncorrelated. In order to distinguish the correlation from anti-correlation, one can use the following colour coding for the lines in question:

correlation : ⟷ anti − correlation : ⟷ . (22)

Let us consider a number of prominent rare decays and divide them into two classes:

Class A: Decays that are governed by vector ($V = \gamma_\mu$) quark couplings. These are, for instance,

$$K^+ \to \pi^+ \nu\bar{\nu}\,, \qquad K_L \to \pi^0 \nu\bar{\nu}\,, \qquad B \to K \nu\bar{\nu}\,, \qquad B \to K \mu^+ \mu^-\,. \quad (23)$$

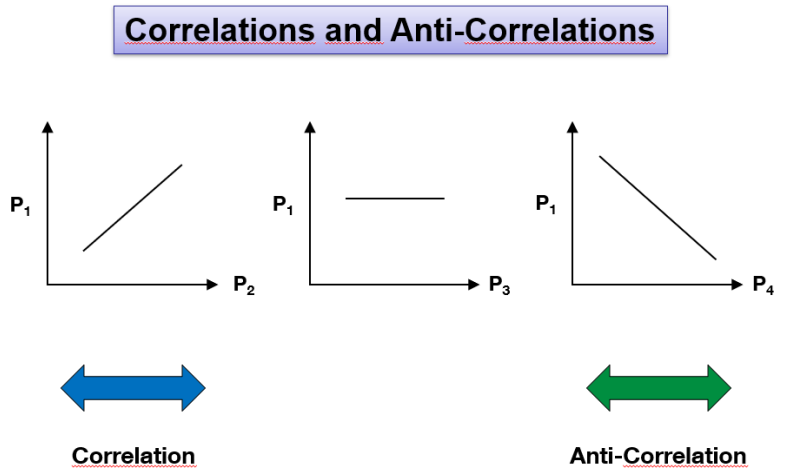

Fig. 15. Correlations, no correlations, and anti-correlation. P_i is the probability representing the branching ratio in public colloquia.

In this case, the change from left-handed to right-handed quark couplings does not introduce any change in the sign of NP contribution relatively to the SM one.

Class B: Decays that are governed by axial-vector ($A = \gamma_\mu\gamma_5$) quark couplings. These are, for instance,

$$K_{\rm L} \to \mu^+\mu^-\,, \qquad B \to K^*\nu\bar{\nu}\,, \qquad B_{s,d} \to \mu^+\mu^-\,, \qquad B_d \to K^*\mu^+\mu^-\,. \tag{24}$$

In this case, the change from left-handed to right-handed couplings implies the sign flip of the NP contribution relatively to the SM one. Strictly speaking, in the case of $B \to K^*\nu\bar{\nu}$ and $B_d \to K^*\mu^+\mu^-$, this rule only applies if the contributions from the longitudinal and parallel transversity components dominate. For the perpendicular component, there is no sign flip.

Thus, if there is a correlation between two observables, one belonging to class A and the other to class B, in the presence of left-handed couplings, it is changed into anti-correlation when right-handed couplings are at work. This difference allows then to probe whether one deals with left-handed or right-handed couplings. Of course, if both left-handed and right-handed couplings are involved, the structure of correlations is modified, but still, studying it, one can in principle extract the relative size of these couplings from the data. Moreover, if there is a correlation or anti-correlation of two observables belonging to one class, the flip of the sign of γ_5 will not have an impact on these relations, but can, of course, have an impact on whether a given observable is suppressed or enhanced relative to the SM prediction.

A graphical representation of these properties are the DNA charts [56] which we will briefly discuss now. Let me then end this description with four charts presented in [56], where further details can be found.

One can check that these charts summarize compactly the (anti-) correlations between processes of class A and B that we discussed before, and also the correlations and anti-correlations within each class. In particular, the change of a correlation into an anti-correlation between two observables belonging to two different classes, when left-handed couplings are changed to right-handed ones, are clearly visible in these charts. We observe the following features:

— Comparing the DNA charts of CMFV and $\mathrm{U}(2)^3$ models in Fig. 16, we observe that the correlations between K and $B_{s,d}$ systems are absent in the $\mathrm{U}(2)^3$ case as the flavour symmetry is reduced from $\mathrm{U}(3)^3$ down to $\mathrm{U}(2)^3$.

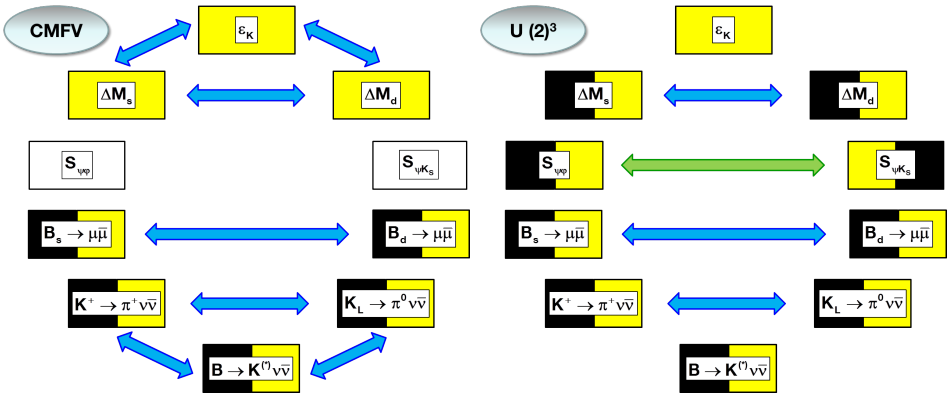

Fig. 16. DNA chart of MFV models (left) and of $\mathrm{U}(2)^3$ models (right). Yellow means enhancement, black means **suppression**, and white means no change. Blue arrows $\Leftrightarrow$ indicate correlation, and green arrows $\Leftrightarrow$ indicate anti-correlation. From [56].

— As the $K^+ \to \pi^+ \nu\bar{\nu}$, $K_\mathrm{L} \to \pi^0 \nu\bar{\nu}$ and $B \to K \nu\bar{\nu}$ decays belonging to class A are only sensitive to the vector quark currents, they do not change when the couplings are changed from left-handed to right-handed ones. On the other hand, the remaining three decays in Fig. 17 belonging to class B are sensitive to axial-vector couplings implying interchange of enhancements and suppressions when going from L to R and also a change of correlations to anti-correlations between the latter three and the former three decays. Note that the correlation between $B_s \to \mu^+\mu^-$ and $B \to K^*\mu^+\mu^-$ does not change as both decays are

sensitive only to axial-vector coupling if, in the latter case, the contribution from the longitudinal and parallel transversity components dominate.

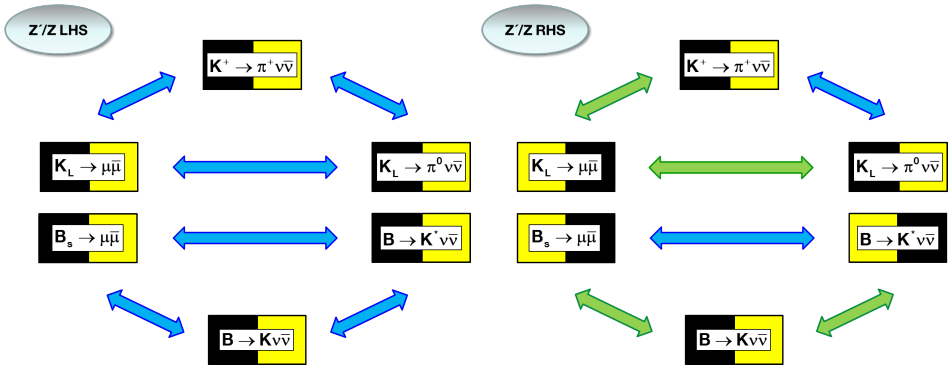

Fig. 17. DNA charts of Z' models with LH and RH currents. Yellow means enhancement, black means **suppression**, and white means no change. Blue arrows $\Leftrightarrow$ indicate correlation and green arrows $\Leftrightarrow$ indicate anti-correlation. From [56].

— However, it should be remarked that in order to obtain the correlations or anti-correlations in the LHS and RHS scenarios it was assumed in the DNA charts presented here that the signs of the left-handed couplings to neutrinos and the axial-vector couplings to muons are the same which does not have to be the case. If they are opposite, the correlations between the decays with neutrinos and muons in the final state change to anti-correlations and *vice versa*.

— On the other hand, due to $\mathrm{SU}(2)_{\mathrm{L}}$ symmetry, the left-handed Z' couplings to muons and neutrinos are equal, and this implies the relation

$$\Delta_{\mathrm{L}}^{\nu\bar{\nu}}\left(Z'\right) = \frac{\Delta_{\mathrm{V}}^{\mu\bar{\mu}}\left(Z'\right) - \Delta_{\mathrm{A}}^{\mu\bar{\mu}}\left(Z'\right)}{2}\,. \tag{25}$$

Therefore, once two of these couplings are determined, the third follows uniquely without the freedom mentioned in the previous item.

— In the context of the DNA charts in Fig. 17, the correlations involving $K_{\mathrm{L}} \to \pi^0\nu\bar{\nu}$ apply only if NP contributions carry some CP-phases. If this is not the case, the branching ratio for $K_{\mathrm{L}} \to \pi^0\nu\bar{\nu}$ will remain unchanged relative to the SM one.

If in the case of tree-level Z' and Z exchanges, both LH and RH quark couplings are present and are equal to each other (LRS scenario) or differ by sign (ALRS scenario), then one finds [58]

— In LRS NP, contributions to $B_{s,d} \to \mu^+\mu^-$ vanish, but they are present in $K_{\rm L} \to \pi^0\nu\bar{\nu}$, $K^+ \to \pi^+\nu\bar{\nu}$, $B_d \to K\mu^+\mu^-$, and $B \to K\nu\bar{\nu}$.

— In ALRS NP, contributions to $B_{s,d} \to \mu^+\mu^-$ are non-vanishing. On the other hand, they are absent in the case of $K_{\rm L} \to \pi^0\nu\bar{\nu}$, $K^+ \to \pi^+\nu\bar{\nu}$, $B_d \to K\mu^+\mu^-$, and $B \to K\nu\bar{\nu}$.

— In $B_d \to K^*\mu^+\mu^-$ and $B \to K^*\nu\bar{\nu}$, this rule is more complicated as already stated above, but generally the LH and RH contributions interfere destructively in LRS and constructively in ALRS. The details depend on form factors.

As described in detail in [59], this strategy can also be presented in a different manner. In Fig. 18, various observables of interest are exposed around the first three clocks. In the last clock, several NP models (theories) are listed for which the first three clocks can be constructed one day.

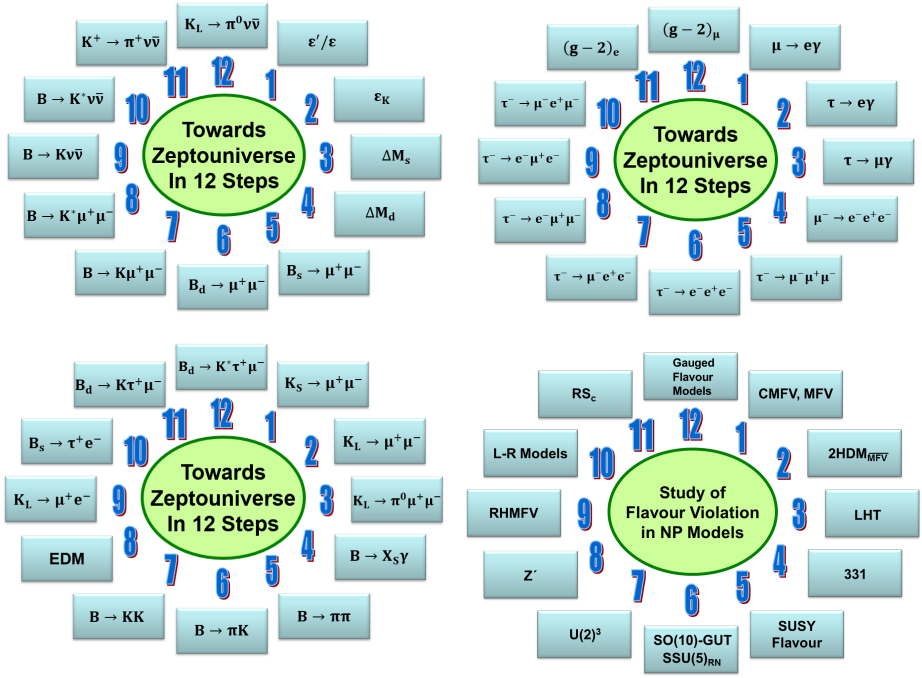

Fig. 18. Towards the zeptouniverse in 12 steps.

This is illustrated in Fig. 19 which shows DNA tests of different theories with enhancements, suppressions, and no changes for specific observables in a given clock of Fig. 18. The last clock in Fig. 19 shows the experimental result for the chosen observables. As one can see, all five theories are ruled out.

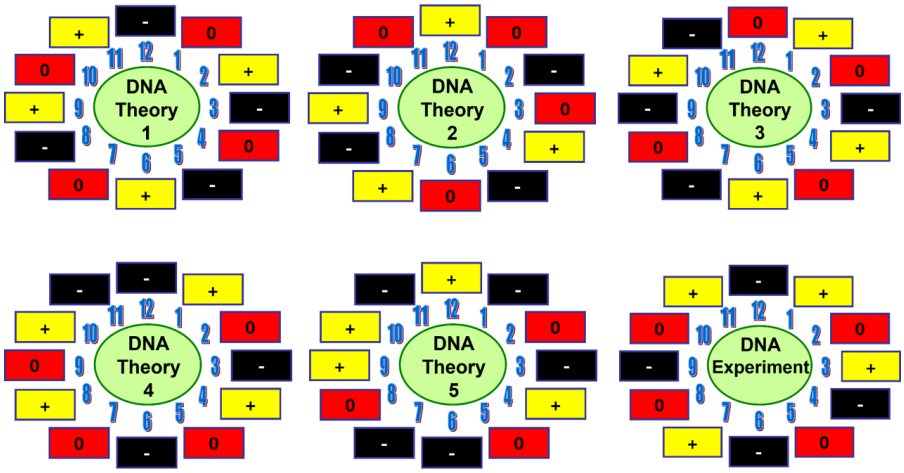

Fig. 19. DNA tests of several theories with the last one being experimental DNA.

Of course, due to free parameters in a given theory, it is seldom that the signs in these clocks are unique. But as in the special NP scenarios presented in Figs. 16 and 17, the signs in question could be correlated. In the future, when many observables will be measured, the clocks presented here, together with the DNA charts, could help to present results in a given theory in an artistic manner.

8. New Physics models

While the strategies for searching for NP are very important, at the end, one has to construct specific models that explain possible anomalies observed in the experimental data. Numerous NP models have been developed in the literature over the last three decades[3]. Many of them have been analyzed in my group at TUM, dominantly in the first two decades of this millennium. They are listed in Fig. 20. The ones with stars were most popular in the literature.

My Ph.D. students and Postdocs contributed in a crucial manner to these analyses. We analyzed all these NP models in detail. This means deriving Feynman Rules, calculating flavour observables, and studying phenomenological implications of these models. In particular, through correlations between different observables.

The atlas of these analyses, with short descriptions of the main results, is presented in Part X of [1] and a more extensive list can be found in chapters 15 and 16 of my book [6]. I will not repeat this list here. Instead, I will present in the next section an album of the correlations between various observables in specific models.

[3] See [61].

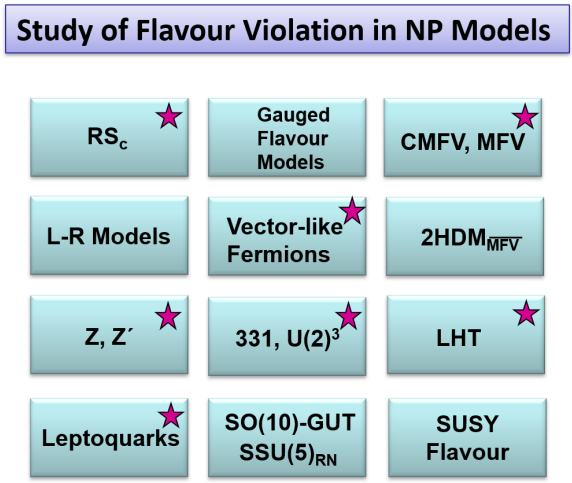

Fig. 20. NP models investigated in my group at TUM.

Personally, I hope that one day, a Z', leptoquarks, and vector-like quarks and leptons will be discovered.

9. Correlations in various NP scenarios

In this section, I show a number of correlations obtained with my Ph.D. students, Postdocs, and other collaborators. I describe them very briefly. A bit longer summaries can be found in my *Flavour Autobiography* [1].

— Figure 21 illustrates common correlations in the $\mathcal{B}(K^+ \to \pi^+ \nu\bar{\nu})$ *versus* $\mathcal{B}(K_{\rm L} \to \pi^0 \nu\bar{\nu})$ plane. The expanding red region illustrates the lack of correlation for models with general LH and RH NP couplings. The green region shows the correlation present in models obeying CMFV. The blue region shows the correlation induced by the constraint from ε_K if only LH or RH couplings are present. From [60].

— Figure 22 presents hypothetical constraints on the ϵ–η plane [63, 64], assuming $\mathcal{B}(B \to K\nu\bar{\nu})$, $\mathcal{B}(B \to K^*\nu\bar{\nu})$, $\mathcal{B}(B \to X_s\nu\bar{\nu})$, and $\langle F_{\rm L}\rangle$ (longitudinal polarization) have been measured with infinite precision. ϵ and η are defined through

$$\epsilon = \frac{\sqrt{\left|C_{\rm L}^{\nu}\right|^2 + \left|C_{\rm R}^{\nu}\right|^2}}{\left|\left(C_{\rm L}^{\nu}\right)^{\rm SM}\right|}\,, \qquad \eta = \frac{-{\rm Re}\left(C_{\rm L}^{\nu} C_{\rm R}^{\nu *}\right)}{\left|C_{\rm L}^{\nu}\right|^2 + \left|C_{\rm R}^{\nu}\right|^2}\,, \tag{26}$$

where $C_{\rm LR}^{\nu}$ are the relevant WCs that enter the expressions for the four observables in question. $\epsilon = 1$ in the SM. A non-vanishing η signals the

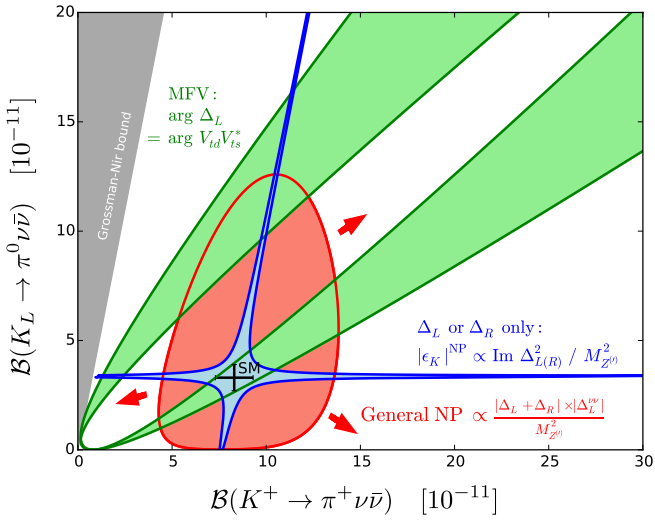

Fig. 21. Illustrations of common correlations in the $\mathcal{B}(K^+ \to \pi^+\nu\bar{\nu})$ *versus* $\mathcal{B}(K_{\rm L} \to \pi^0\nu\bar{\nu})$ plane. See the text for explanations. From [60].

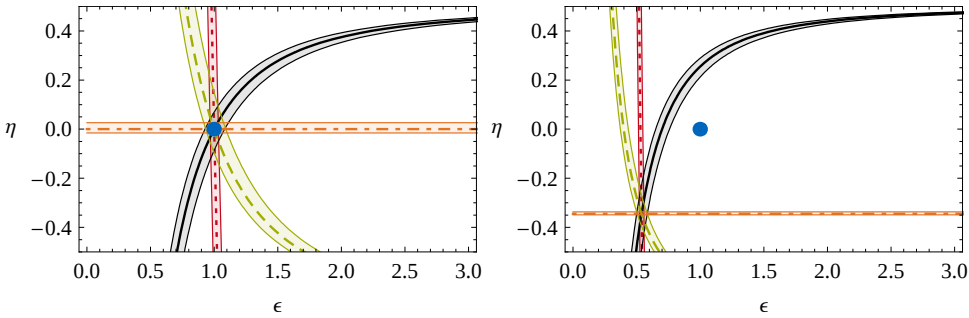

Fig. 22. Hypothetical constraints on the ϵ–η plane, assuming all four observables have been measured with infinite precision. See the text for explanations. From [62].

presence of new right-handed down-quark flavour violating couplings which can be ideally probed by the decays in question. The error bands in Fig. 22 reflect the theoretical uncertainty in 2009. The green band (dashed line) represents $\mathcal{B}(B \to K^*\nu\bar{\nu})$, the black band (solid line) $\mathcal{B}(B \to K\nu\bar{\nu})$, the red band (dotted line) $\mathcal{B}(B \to X_s\nu\bar{\nu})$, and the orange band (dot-dashed line) $\langle F_{\rm L}\rangle$. Left: SM values for the Wilson coefficients. Right: assuming $C_{\rm L}^{\nu} = 0.5(C_{\rm L}^{\nu})^{\rm SM}$ and $C_{\rm R}^{\nu} = 0.2(C_{\rm L}^{\nu})^{\rm SM}$. The blue circle represents the SM point. From [62].

— Using the definitions in (30) and assuming that only vector currents contribute, one finds [65]

$$\mathcal{R}_K = (1-2\,\eta)\epsilon^2\,, \quad \mathcal{R}_{K^*} = (1+\kappa_\eta\eta)\epsilon^2\,, \quad \mathcal{R}_{F_\mathrm{L}} \equiv \frac{F_\mathrm{L}}{F_\mathrm{L}^\mathrm{SM}} = \frac{1+2\eta}{1+\kappa_\eta\eta}\,. \tag{27}$$

The parameter κ_η depends on the form factors.

Since the three observables in (27) only depend on two combinations of Wilson coefficients, there is a model-independent prediction

$$F_\mathrm{L} = F_\mathrm{L}^\mathrm{SM}\left(\frac{(\kappa_\eta-2)\mathcal{R}_K + 4\,\mathcal{R}_{K^*}}{(\kappa_\eta+2)\mathcal{R}_{K^*}}\right). \tag{28}$$

In principle, this relation can be tested experimentally (also on a bin-by-bin basis). A similar relation can be obtained for the modification of the inclusive $B \to X_s\nu\bar{\nu}$ branching ratio

$$\mathrm{BR}(B\to X_s\nu\bar{\nu}) \approx \mathrm{BR}(B\to X_s\nu\bar{\nu})_\mathrm{SM}\left(\frac{\kappa_\eta\mathcal{R}_K + 2\,\mathcal{R}_{K^*}}{\kappa_\eta+2}\right). \tag{29}$$

The generalization of all these relations to the case of lepton universality violation and/or lepton flavour violation have been presented in Section 4.5 of [66]. Once the data on these four observables improves, the sum-rule analysis presented there should offer an important insight into possible NP at work.

— Figure 23 displays $\bar{\mathcal{B}}(B_s \to \mu^+\mu^-)$ *versus* the ratio $\mathcal{B}(B\to K\nu\bar{\nu})/\mathcal{B}(B\to K\nu\bar{\nu})_\mathrm{SM}$ for $\beta = \pm\frac{2}{\sqrt{3}}, \pm\frac{1}{\sqrt{3}}$ that distinguishes between various 331 models. Colours describe different values of $\Delta M_s/(\Delta M_s)_\mathrm{SM}$. From [67].

— Figure 24 from [65] displays various correlations between observables in LHS (red), RHS (blue), LRS (green), ALRS (yellow), assuming LFU and $\Delta_\mathrm{R}^{\nu\nu} = \Delta_\mathrm{R}^{\ell\ell} = 0$. All points satisfy $0.9 \le \Delta M_s/(\Delta M_s)_\mathrm{SM} \le 1.1$, $-0.14 \le S_{\psi\phi} \le 0.14$. Grey regions are disfavoured at 2σ by $b\to s\mu^+\mu^-$ constraints in 2014. All ratios are defined by

$$\mathcal{R}_{K(K^*)} = \frac{\mathcal{B}(B\to K(K^*)\nu\bar{\nu})}{\mathcal{B}(B\to K(K^*)\nu\bar{\nu})_\mathrm{SM}}\,, \quad \mathcal{R}_{K(K^*)\mu\mu} = \frac{\mathcal{B}(B\to K(K^*)\mu\bar{\mu})}{\mathcal{B}(B\to K(K^*)\mu\bar{\mu})_\mathrm{SM}}, \tag{30}$$

and $\mathcal{R}_{\mu\mu}$ for $B_s \to \mu\bar{\mu}$. The 2024 update of these correlations has been presented in [68] and is summarized in [1].

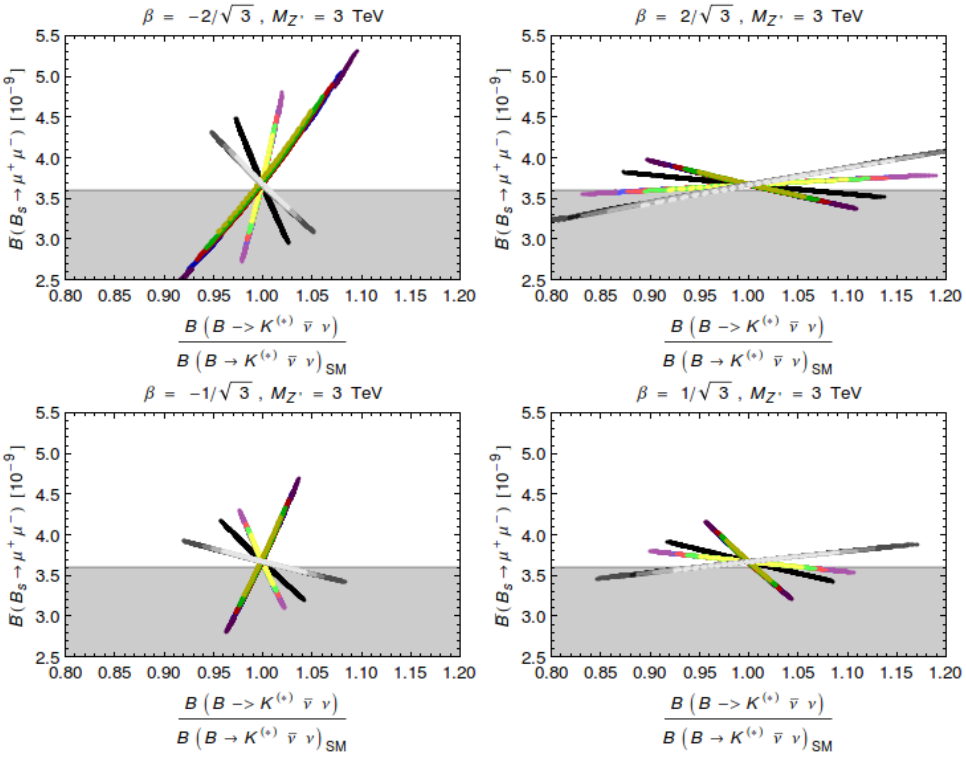

Fig. 23. $\bar{\mathcal{B}}(B_s \to \mu^+\mu^-)$ *versus* the $\mathcal{B}(B \to K\nu\bar{\nu})/\mathcal{B}(B \to K\nu\bar{\nu})_{\rm SM}$ ratio for all four $\beta = \pm\frac{2}{\sqrt{3}}, \pm\frac{1}{\sqrt{3}}$. Colours describe different values of $\Delta M_s/(\Delta M_s)_{\rm SM}$. From [67].

— Figure 25 shows $\mathcal{B}(K^+ \to \pi^+\nu\bar{\nu})$–$\mathcal{B}(K_{\rm L} \to \pi^0\nu\bar{\nu})$ plane for vector-current contributions with $C_{\rm S} = 0$ (top) and scalar-current contributions with $C_{\rm V} = 0$ (bottom) assuming lepton–flavour universality. The phase $\phi_{\rm V}$ (ϕ_S) is fixed to different values (see legend) and $C_{\rm V}$ ($C_{\rm S}$), the size of vector (scalar) contributions is varied. The red line indicates the Grossmann–Nir bound. The SM contribution is represented by a black point. The grey region represents the present experimental 1σ range. See [66] for details.

— Figure 26 displays $\mathcal{B}(K_{\rm L} \to \pi^0\nu\bar{\nu})$ *versus* $\mathcal{B}(K^+ \to \pi^+\nu\bar{\nu})$ for $M_{Z'} = 50$ TeV in the LHS (left) and for $M_{Z'} = 500$ TeV in the L+R scenario. The colours distinguish between different CKM input considered by us which also implies the four red points corresponding to the SM central values for these four CKM scenarios. The black line corresponds to the Grossman–Nir bound [69]. The gray region shows the experimental range of $\mathcal{B}(K^+ \to \pi^+\nu\bar{\nu}))_{\rm exp} = (17.3^{+11.5}_{-10.5}) \times 10^{-11}$ known in 2014 [70].

With the improved value in Table 2, this region is by a factor of 2.5 smaller. This paper illustrates that very high energy scales can be resolved with the help of rare Kaon decays. It will be interesting to repeat this analysis one day when the experimental data improve.

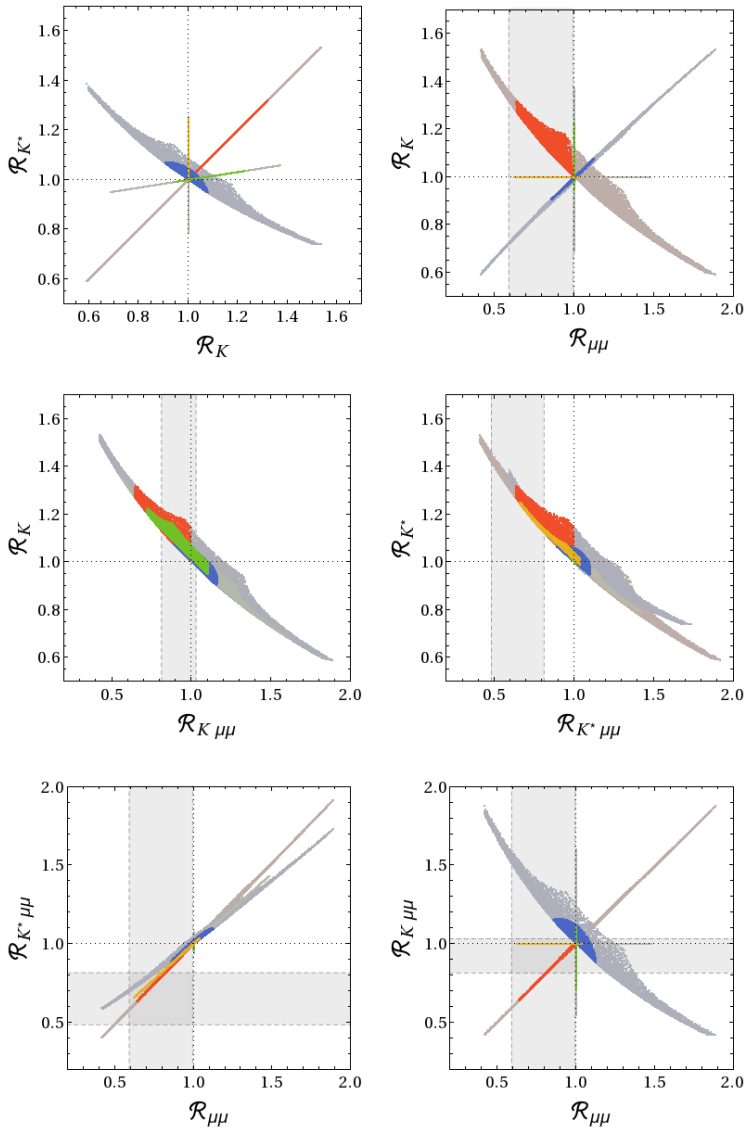

Fig. 24. Various correlations between observables in LHS (red), RHS (blue), LRS (green), ALRS (yellow), assuming LFU and $\Delta_{\mathrm{R}}^{\nu\nu} = \Delta_{\mathrm{R}}^{\ell\ell} = 0$. From [65]. Update in [68].

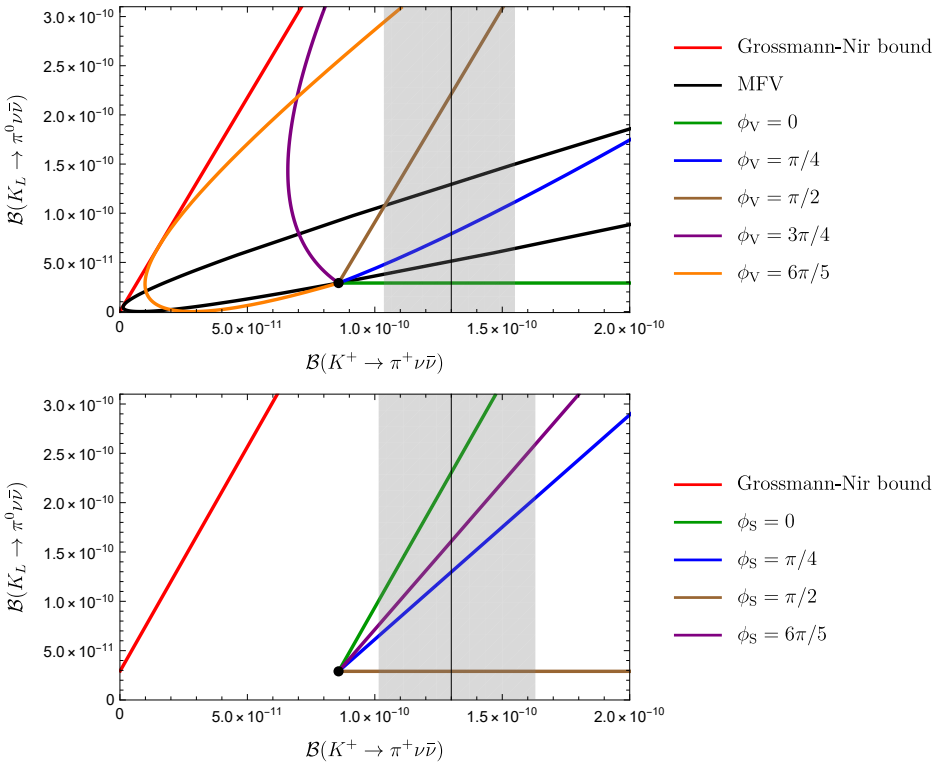

Fig. 25. $\mathcal{B}(K^+ \to \pi^+\nu\bar{\nu})$–$\mathcal{B}(K_L \to \pi^0\nu\bar{\nu})$ plane for vector-current contributions with $C_S = 0$ (top) and scalar-current contributions with $C_V = 0$ (bottom) [66].

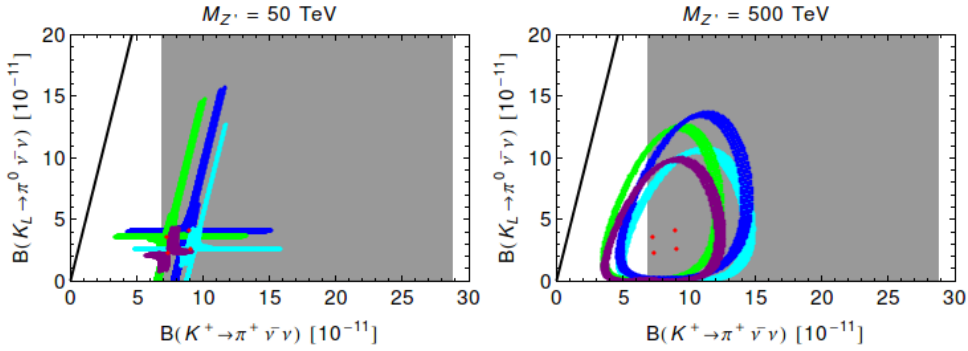

Fig. 26. $\mathcal{B}(K_L \to \pi^0\nu\bar{\nu})$ *versus* $\mathcal{B}(K^+ \to \pi^+\nu\bar{\nu})$ for $M_{Z'} = 50$ TeV in the LHS (left) and for $M_{Z'} = 500$ TeV in the L+R scenario. From [70].

— Figure 27 displays the $\mathcal{B}(B^+ \to K^+\nu\widehat{\nu})$–$\mathcal{B}(B \to K^*\nu\widehat{\nu})$ plane (top) and $\mathcal{B}(B \to K_{\rm L}^*\nu\widehat{\nu})$–$\mathcal{B}(B \to K_{\rm T}^*\nu\widehat{\nu})$ plane (bottom) for different NP scenarios as described in the figure caption (see [66] for details).

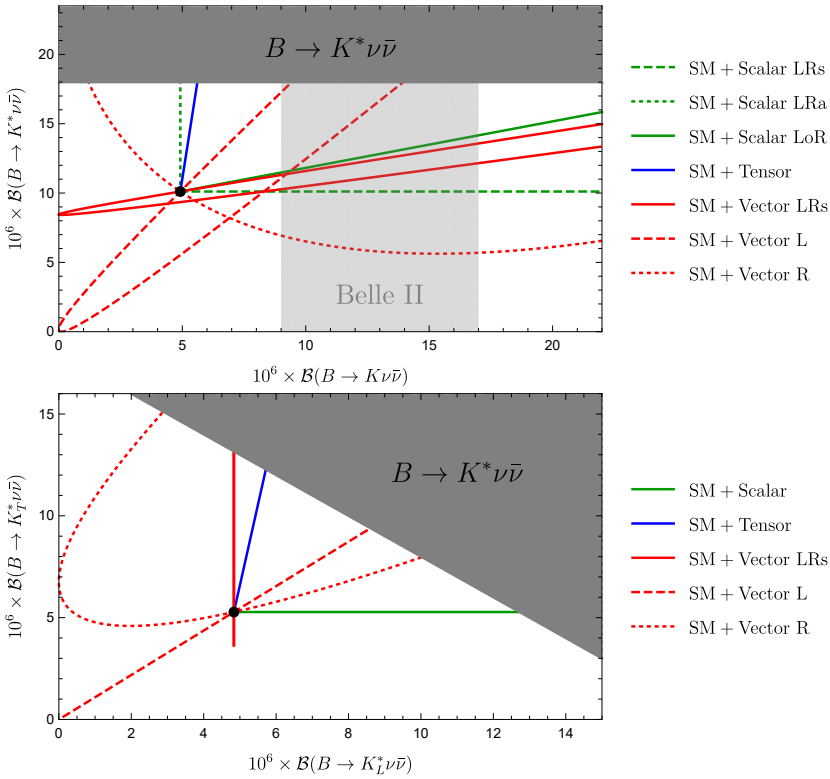

Fig. 27. The figure displays the $\mathcal{B}(B^+ \to K^+\nu\widehat{\nu})$–$\mathcal{B}(B \to K^*\nu\widehat{\nu})$ plane (top) and $\mathcal{B}(B \to K_{\rm L}^*\nu\widehat{\nu})$–$\mathcal{B}(B \to K_{\rm T}^*\nu\widehat{\nu})$ plane (bottom) for different NP scenarios [66]. The SM predictions are represented by black points. The light gray region in the upper plot indicates the 2023 experimental range quoted from Belle II [52], and the dark gray regions are excluded by the experimental limit on $B \to K^*\widehat{\nu}\nu$. The green lines show NP scenarios with scalar currents, the blue lines NP scenarios with tensor currents, and the red curves NP scenarios with vector currents.

— Figure 28 shows the correlations between the observable $R^+_{\nu\bar{\nu}}$ and various other Kaon observables in a Z' model with the imaginary $Z\bar{s}d$ coupling implying no NP contributions to ε_K. All ratios $R_i = 1$ in the SM. Note that for $K_{\rm L} \to \pi^0\nu\bar{\nu}$ and $K_{\rm S} \to \mu^+\mu^-$, the ratios are divided by 10 and, 25 respectively. From [71].

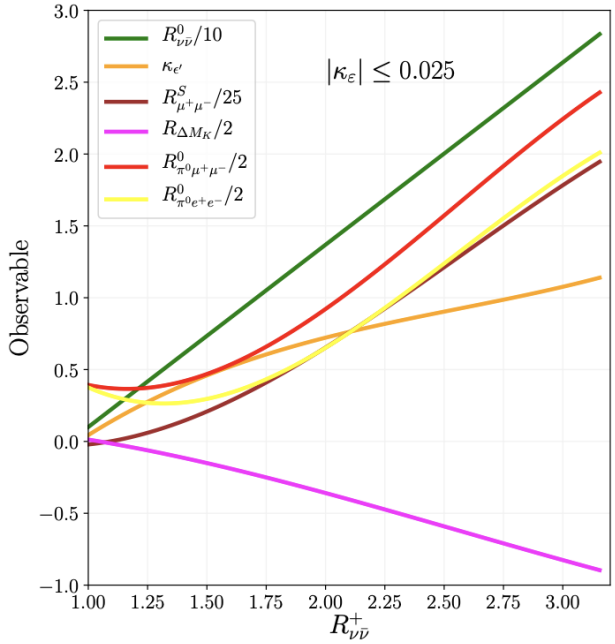

Fig. 28. Correlations between the observable $R^+_{\nu\bar{\nu}}$ and various other Kaon observables in a Z' model. See the text for explanations. From [71].

Table 3. References to correlations between observables in various NP models studied in my group.

Model	Reference	Model	Reference
CMFV	[35, 74–76]	RHMFV	[94]
$U(2)^3$	[60, 77]	RSc	[95, 96]
$2HDM_{\overline{MFV}}$	[78, 79]	Minimal Theory of Fermion Masses	[97]
ACD model	[80, 81]	Z'	[58, 65, 68, 71]
LH	[82, 83]	331	[67, 98, 99]
LHT	[84–86]	Scalars	[100, 101]
SM4	[87–89]	Leptoquarks	[102]
AC, RVV2, AMK, δLL	[90, 91]	VLQ	[103]
$SSU(5)_{RN}$	[92]	SMEFT	[27]
FBMSSM	[93]		

In Table 3, the references to papers from my group that analyzed various correlations in several NP scenarios have been collected for convenience. The more general strategies like the ones with Jennifer [56] and Elena [34, 44, 72] have not been listed there. While the last entry in this table is our recent SMEFT review [27] in which such correlations have been described systematically, several analyses listed in this table were performed in the framework of the SMEFT. This is in particular the case of [65, 73] and [68].

10. SMEFT correlations between flavour observables

10.1. Preface

As we have seen in the previous section, several processes are correlated within a given NP model through various flavour and gauge symmetries present in this model. However, independently of such symmetries specific to a given model, additional correlations between observables are generated through operator mixing in the process of RG evolution. This often has an important impact on phenomenology as is evident from the analyses listed in Table 3 and the SMEFT review [27]. The importance of RG effects has also been reemphasized in [104]. Here, we just mention two examples investigated in detail in the literature.

First, the explanation of the so-called B-physics anomalies in semi-leptonic B decays with leptoquarks implies new effects in Lepton Flavour Violating (LFV) decays, thereby putting significant bounds on the coefficients of semi-leptonic operators as stressed in particular in [105, 106].

Similarly, the attempt to obtain significant enhancement of the ratio ε'/ε within leptoquark models [102] is very much restricted by rare Kaon decays.

Generally, such correlations are within processes of a given type such as semi-leptonic, non-leptonic, and leptonic ones. But as exemplified above and discussed at length in [27], they can take place between different types of processes.

In the following, we will elaborate briefly on various origins of correlations that are found in an effective theory at different stages of the analysis. Much more extensive analysis with tables can be found in the SMEFT review in [27].

10.2. Type of correlations in the SMEFT

Correlations through common WCs at tree-level

First of all there are correlations when a given WC enters two or more observables and varying its value changes the predictions of these observables in a correlated manner. Tables 17–19 in [27] indicate which classes of observables are correlated in this manner. These are the strongest correlations between observables.

$\mathrm{SU(2)_L}$ correlations at tree-level

Next, there are correlations due to $\mathrm{SU(2)_L}$ gauge symmetry. Choosing a value of a given $C_i(\Lambda)$ implies a value of another $C_j(\Lambda)$ that is related to $C_i(\Lambda)$ by the unbroken $\mathrm{SU(2)_L}$ gauge symmetry. Numerous tables in [27] indicate which classes of observables are correlated in this manner. In particular, the decays governed by transitions $b \to s\mu^+\mu^-$ and $b \to s\nu\bar{\nu}$ are correlated in this manner and the same applies to $s \to d\mu^+\mu^-$ and $s \to d\nu\bar{\nu}$. Also, such correlations are strong.

Operator mixing due to gauge interactions

When RG evolution is performed from the NP scale $\Lambda_{\rm NP}$ down to $\mu_{\rm ew}$ and subsequently to $\mu_{\rm had}$, new operators enter the game that were not active at the NP scale. They can modify the correlations present already at tree-level but could also lead to new correlations between observables that were absent at tree-level. Being suppressed by gauge couplings, they are generally smaller than at tree-level except of course for those which were absent at tree-level. But in the case of large anomalous dimensions (ADMs) of involved operators, they can still have a significant impact on the phenomenology through large logarithms multiplying the gauge couplings. Again, in [27], it is indicated which classes of observables are correlated in this manner.

Operator and flavour mixing due to top-quark Yukawas

Of particular importance is the impact of the top-quark Yukawa coupling, both on the operator mixing like in the case of gauge interactions but in addition due to flavour mixing absent in the latter case. In particular, when starting the RG evolution at $\Lambda_{\rm NP}$ in a given flavour basis in which either the up-quark Yukawa matrix $\hat{Y}_u$ or the down-quark Yukawa matrix $\hat{Y}_d$ is diagonal, one finds that at $\mu_{\rm ew}$ after the RG evolution, these matrices, being respectively diagonal at $\Lambda_{\rm NP}$, are no longer diagonal. A back-rotation [107] has to be performed to make these matrices diagonal at $\mu_{\rm ew}$. This can also have an impact not only on the values of WCs but also on correlations between different observables.

Matching effects

Also, the matching between a UV completion and the SMEFT, as well as the matching between the SMEFT and the WET, can have an impact on the correlations between various observables. It can be significant but in contrast to RG effects, it is not enhanced by large logarithms of the type $\ln \Lambda_{\rm NP}/\mu_{\rm ew}$. This applies both to the tree-level matching and to one-loop matching. The inclusion of the latter is required in particular at the NLO level of an RG analysis to cancel the unphysical renormalization scheme dependencies of two-loop anomalous dimensions and also various scale dependencies.

Modification of SM parametrs through dim-6 operators

Finally, the correlations in question can enter through $1/\Lambda^2$ effects on the SM parameters.

This list of possible dynamical effects makes it clear that to find the correlations between observables, within the SMEFT computer codes are indispensable. Fortunately, there exist a number of very efficient codes on the market [108] that can perform this task. The listing of these codes with brief explanations can be found in Section 10 of [27].

However, no numerical analysis of the correlations in question has been performed in [27]. Presently, two numerical analyses are in progress. There is a chance that at least one of them will be completed by June this year.

11. Summary, shopping list and outlook

11.1. Summary

Despite the presence of various anomalies in the existing data, it is clearly not evident which animalcula could be responsible for them. On the basis of the studies I have been involved in, possibly the main candidates are Z' vector bosons, leptoquarks, vector-like quarks, and vector-like leptons but to find out without any doubts what they are we need more data, in particular for theoretically clean decays as the ones listed in Table 2. Precise measurements of branching ratios for these decays and of various kinematical distributions should allow us in this decade and the next decade to find out which animalcula are responsible for them. The strategies presented in this paper and also discussed in more detail in [1] should be helpful in this respect. It should be stressed that the ratios listed in Section 6 test the SM independently of whether NP effects are strongly suppressed in $\Delta F = 2$ processes or not. Having several measurements of these ratios and seeing some pattern in deviations from their SM predictions would already be very exciting. One could then return to the strategies like the DNA one of Section 7 and other strategies involving correlations between observables. In particular, updated studies of explicit models listed in Fig. 20 could be very helpful in identifying the candidates for a UV completion.

11.2. Shopping list

Let me next present my shopping list for the coming years. A much more detailed list can be found in Chapter 20 of my book [6]. I list here only the entries related to indirect searches for NP, in particular, flavour physics. There is no question about that discovering a new particle at the LHC would be most exciting as this would reduce the number of possible extensions of the SM by much. Here comes my shortened shopping list.

1. Precise measurements of the branching ratios for the 7 magnificent decays listed in Table 2, and as studied in [66], of missing energy distributions for four decays among them. Presently, on a forefront are the $B \to K^{(*)}\nu\bar{\nu}$ decays studied intensively by the Belle II experiment [52], giving some hints for NP contributions. There are very many recent analyses of these data. A collection of references to these analyses can be found in [27] but surely some have been performed since then. The same applies to $K^+ \to \pi^+\nu\bar{\nu}$ for which a very interesting result has been provided by the NA62 experiment listed in Table 2. A new one should be available this or next year. I am looking forward to the improved determination of the ratios in (9) and (11). As seen in (17), the first one is consistent with the SM but could still differ from it when a more accurate measurement from NA62 will be known. On the other hand, as seen in (18), the ratio (11) differs significantly from the precise SM prediction.

2. Precise measurements of the branching ratios and of other observables in $B \to K\ell^+\ell^-$ and $B \to K^*\ell^+\ell^-$ decays [110] and the clarification of the anomalies in them.

3. Precise measurements of $|V_{cb}|$ and γ in tree-level decays that would provide additional tests of the BV-strategy of Section 6. In this context, the $(|V_{cb}|, \gamma)$ plots in Fig. 29 could help to identify the presence of NP.

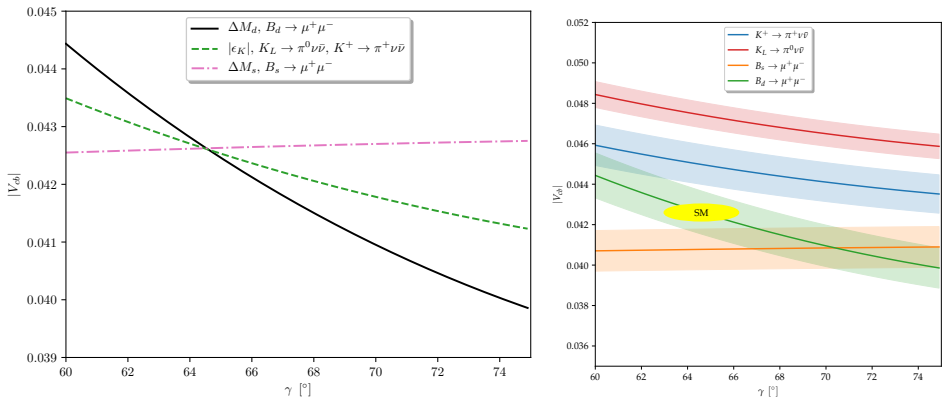

Fig. 29. Left: Schematic illustration of the action of the seven observables in the $|V_{cb}|$–γ plane in the context of the SM. We set $\beta = 22.2°$ and all uncertainties to zero. Right: The impact of hypothetical future measurements of the branching ratios for $K^+ \to \pi^+\nu\bar{\nu}$, $K_{\rm L} \to \pi^0\nu\bar{\nu}$, $B_d \to \mu^+\mu^-$, and $B_s \to \mu^+\mu^-$ on the $|V_{cb}|$–γ plane. All uncertainties are included. The yellow disc represents the SM. From [109].

4. Clarification of anomalies in $B \to \pi K$ decays [111–116] and continuation of the intensive studies of several other $B \to PP$ decays with $B = B^0_{d,s}, B^+$ and $P = \pi, K, K^*$.

5. Completion of the calculations of ε'/ε and of the $\Delta I = 1/2$ rule by the RBC-UKQCD Lattice QCD Collaboration and of corresponding calculations by another Lattice QCD group with $2+1+1$ flavours. In particular, the isospin breaking contributions to QCD penguins are still missing in present lattice results for ε'/ε. As stressed in [48], Jean-Marc Gérard and I expect, on the basis of DQCD developed with Bill Bardeen, significant NP contributions to ε'/ε.

6. Calculation of hadronic matrix elements relevant for ΔM_s and ΔM_d with $2+1+1$ flavours by other Lattice QCD collaborations in order to check HPQCD results [41] for these matrix elements.

7. Further searches for lepton flavour violation and EDMs.

11.3. Outlook

Assuming that at least few of these entries will be realized in the coming 20 years, in particular, the one on ε'/ε, we should have then a great time until 2046 and this is expressed in Fig. 30.

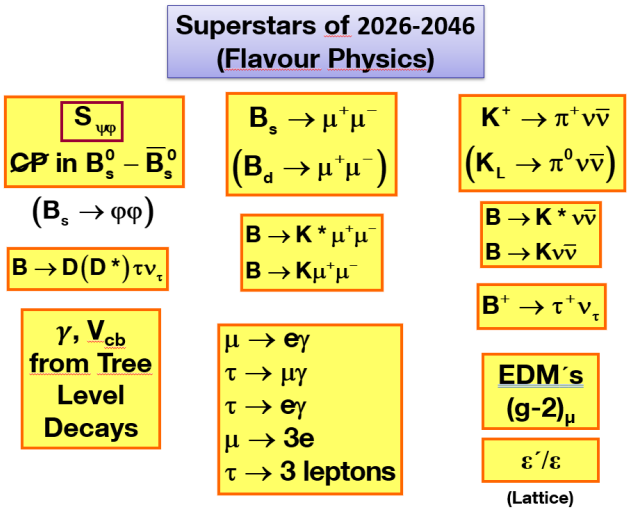

Fig. 30. Coming years.

Unfortunately, it could take longer. After all, Enrico Fermi, already in the 1930s, could sense something going on which was hidden in his G_F. But it took the first 30 years to suggest that it could be a heavy gauge boson $W^\pm$ behind these effects, and another 20 years to discover it. Let us hope that it will not take such a long time now and that we will be able to narrow the number of possible extensions of the SM at least through indirect searches until 2046. The methods presented here and in [1] will hopefully play an important role in these searches. But from today's perspective, it is difficult to predict how our field will develop in the coming decades. Indeed, let me cite Niels Bohr: "Prediction is very difficult, especially if it's about the future".

I would like to thank Michał Praszałowicz for inviting me to the Cracow School of 2026. Many thanks go to my collaborators to whom my *Flavour Autobiography* [1] is dedicated. Financial support by the Excellence Cluster ORIGINS, funded by the Deutsche Forschungsgemeinschaft (DFG, German Research Foundation), Excellence Strategy, EXC-2094, 390783311 is acknowledged.

REFERENCES

[1] A.J. Buras, «Addicted to Flavour: 1976–2026», arXiv:2601.03722 [hep-ph].

[2] A.J. Buras, «Flavour Theory: 2009», *PoS* **(EPS-HEP2009)**, 024 (2009), arXiv:0910.1032 [hep-ph].

[3] K.G. Wilson, «Non-Lagrangian Models of Current Algebra», *Phys. Rev.* **179**, 1499 (1969).

[4] W. Zimmermann, «Normal products and the short distance expansion in the perturbation theory of renormalizable interactions», *Ann. Phys.* **77**, 570 (1973).

[5] K.G. Wilson, W. Zimmermann, «Operator product expansions and composite field operators in the general framework of quantum field theory», *Commun. Math. Phys.* **24**, 87 (1972).

[6] A.J. Buras, «Gauge Theory of Weak Decays: The Standard Model and the Expedition to New Physics Summits», *Cambridge University Press*, 2020.

[7] A.J. Buras, «Weak Hamiltonian, CP Violation and Rare Decays», in: «Probing the Standard Model of Particle Interactions. Proceedings of Summer School in Theoretical Physics», 68$^{\text{th}}$ session, *NATO Advanced Study Institute*, Les Houches, France, July 28–September 5, 1997, pp. 281–539, arXiv:hep-ph/9806471.

[8] A.J. Buras, «Climbing NLO and NNLO Summits of Weak Decays: 1988–2023», *Phys. Rep.* **1025**, 1 (2023), arXiv:1102.5650 [hep-ph].

[9] Flavour Lattice Averaging Group (FLAG) (Y. Aoki *et al.*), «FLAG Review 2021», *Eur. Phys. J. C* **82**, 869 (2022), arXiv:2111.09849 [hep-lat].

[10] V. Cirigliano *et al.*, «Kaon decays in the standard model», *Rev. Mod. Phys.* **84**, 399 (2012), arXiv:1107.6001 [hep-ph].

[11] HPQCD Collaboration (W.G. Parrott, C. Bouchard, C.T.H. Davies), «$B \to K$ and $D \to K$ form factors from fully relativistic lattice QCD», *Phys. Rev. D* **107**, 014510 (2023), arXiv:2207.12468 [hep-lat].

[12] HPQCD Collaboration (W.G. Parrott, C. Bouchard, C.T.H. Davies), «Standard Model predictions for $B \to K\ell^+\ell^-$, $B \to K\ell_1^-\ell_2^+$ and $B \to K\nu\bar{\nu}$ using form factors from $N_f = 2+1+1$ lattice QCD», *Phys. Rev. D* **107**, 014511 (2023), arXiv:2207.13371 [hep-ph].

[13] W. Parrott, C. Bouchard, C.T.H. Davies, «The search for new physics in $B \to K\ell^+\ell^-$ and $B \to K\nu\bar{\nu}$ using precise lattice QCD form factors», *PoS* **(LATTICE2022)**, 421 (2023), arXiv:2210.10898 [hep-lat].

[14] A. Khodjamirian, B. Melić, Y.-M. Wang, «A guide to the QCD light-cone sum rules for b-quark decays», *Eur. Phys. J. Spec. Top.* **233**, 271 (2024), arXiv:2311.08700 [hep-ph].

[15] S. Jäger, J. Martin Camalich, «On $B \to V\ell\ell$ at small dilepton invariant mass, power corrections, and new physics», *J. High Energy Phys.* **2013**, 43 (2013), arXiv:1212.2263 [hep-ph].

[16] S. Jäger, J. Martin Camalich, «Reassessing the discovery potential of the $B \to K^*\ell^+\ell^-$ decays in the large-recoil region: SM challenges and BSM opportunities», *Phys. Rev. D* **93**, 014028 (2016), arXiv:1412.3183 [hep-ph].

[17] N. Gubernari, D. van Dyk, J. Virto, «Non-local matrix elements in $B_{(s)} \to \{K^{(*)}, \phi\}\ell^+\ell^-$», *J. High Energy Phys.* **2021**, 088 (2021), arXiv:2011.09813 [hep-ph].

[18] M. Ciuchini *et al.*, «Constraints on lepton universality violation from rare B decays», *Phys. Rev. D* **107**, 055036 (2023), arXiv:2212.10516 [hep-ph].

[19] N. Gubernari, M. Reboud, D. van Dyk, J. Virto, «Improved theory predictions and global analysis of exclusive $b \to s\mu^+\mu^-$ processes», *J. High Energy Phys.* **2022**, 133 (2022), arXiv:2206.03797 [hep-ph].

[20] N. Gubernari, M. Reboud, D. van Dyk, J. Virto, «Dispersive analysis of $B \to K^{(*)}$ and $B_s \to \phi$ form factors», *J. High Energy Phys.* **2023**, 153 (2023); *Erratum ibid.* **2025**, 125 (2025).

[21] G. Isidori, Z. Polonsky, A. Tinari, «Explicit estimate of charm rescattering in $B^0 \to K^0\bar{\ell}\ell$», *Phys. Rev. D* **111**, 093007 (2025), arXiv:2405.17551 [hep-ph].

[22] R. Frezzotti *et al.*, «Theoretical framework for lattice QCD computations of $B \to K\ell^+\ell^-$ and $B_s \to \ell^+\ell^-\gamma$ decays rates, including contributions from charming penguin diagrams», *Phys. Rev. D* **113**, 034509 (2026), arXiv:2508.03655 [hep-lat].

[23] W. Buchmüller, D. Wyler, «Effective lagrangian analysis of new interactions and flavor conservation», *Nucl. Phys. B* **268**, 621 (1986).

[24] B. Grzadkowski, M. Iskrzyński, M. Misiak, J. Rosiek, «Dimension-six terms in the Standard Model Lagrangian», *J. High Energy Phys.* **2010**, 085 (2010), arXiv:1008.4884 [hep-ph].

[25] I. Brivio, M. Trott, «The standard model as an effective field theory», *Phys. Rep.* **793**, 1 (2019), arXiv:1706.08945 [hep-ph].

[26] G. Isidori, F. Wilsch, D. Wyler, «The standard model effective field theory at work», *Rev. Mod. Phys.* **96**, 015006 (2024), arXiv:2303.16922 [hep-ph].

[27] J. Aebischer, A.J. Buras, J. Kumar, «SMEFT ATLAS: The Landscape Beyond the Standard Model», arXiv:2507.05926 [hep-ph].

[28] E.E. Jenkins, A.V. Manohar, M. Trott, «Renormalization group evolution of the Standard Model dimension six operators I: formalism and λ dependence», *J. High Energy Phys.* **2013**, 87 (2013), arXiv:1308.2627 [hep-ph].

[29] E.E. Jenkins, A.V. Manohar, M. Trott, «Renormalization group evolution of the Standard Model dimension six operators II: Yukawa dependence», *J. High Energy Phys.* **2014**, 035 (2014), arXiv:1310.4838 [hep-ph].

[30] R. Alonso, E.E. Jenkins, A.V. Manohar, M. Trott, «Renormalization group evolution of the Standard Model dimension six operators III: gauge coupling dependence and phenomenology», *J. High Energy Phys.* **2014**, 159 (2014), arXiv:1312.2014 [hep-ph].

[31] E.E. Jenkins, A.V. Manohar, P. Stoffer, «Low-energy effective field theory below the electroweak scale: operators and matching», *J. High Energy Phys.* **2018**, 16 (2018); *Erratum ibid.* **2023**, 43 (2023), arXiv:1709.04486 [hep-ph].

[32] G. Finauri, P. Gambino, «The q^2 moments in inclusive semileptonic B decays», *J. High Energy Phys.* **2024**, 206 (2024), arXiv:2310.20324 [hep-ph].

[33] M. Blanke, A.J. Buras, «Emerging ΔM_d-anomaly from tree-level determinations of $|V_{cb}|$ and the angle γ», *Eur. Phys. J. C* **79**, 159 (2019), arXiv:1812.06963 [hep-ph].

[34] A.J. Buras, E. Venturini, «Searching for New Physics in Rare K and B Decays without $|V_{cb}|$ and $|V_{ub}|$ Uncertainties», *Acta Phys. Pol. B* **53**, 6 (2022), arXiv:2109.11032 [hep-ph].

[35] A.J. Buras, «Relations between $\Delta M_{s,d}$ and $B_{s,d} \to \mu^+\mu^-$ in models with minimal flavor violation», *Phys. Lett. B* **566**, 115 (2003), arXiv:hep-ph/0303060.

[36] Particle Data Group (P.A. Zyla *et al.*), «Review of Particle Physics», *Prog. Theor. Exp. Phys.* **2020**, 083C01 (2020).

[37] Heavy Flavor Averaging Group (HFLAV) (S. Banerjee *et al.*), «Averages of b-hadron, c-hadron, and τ-lepton properties as of 2023», *Phys. Rev. D* **113**, 012008 (2026), arXiv:2411.18639 [hep-ex].

[38] Flavour Lattice Averaging Group (S. Aoki *et al.*), «FLAG Review 2019», *Eur. Phys. J. C* **80**, 113 (2020), arXiv:1902.08191 [hep-lat].

[39] M. Gorbahn, S. Jäger, S. Kvedaraitė, «RI-(S)MOM to $\overline{\text{MS}}$ conversion for B_K at two-loop order», *J. High Energy Phys.* **2025**, 11 (2025), arXiv:2411.19861 [hep-ph].

[40] Flavour Lattice Averaging Group (S. Aoki *et al.*), «FLAG Review 2021», *Eur. Phys. J. C* **82**, 869 (2022), arXiv:2111.09849 [hep-lat].

[41] R.J. Dowdall *et al.*, «Neutral B-meson mixing from full lattice QCD at the physical point», *Phys. Rev. D* **100**, 094508 (2019), arXiv:1907.01025 [hep-lat].

[42] Heavy Flavor Averaging Group (HFAG) (Y. Amhis *et al.*), «Averages of b-hadron, c-hadron, and τ-lepton properties as of summer 2016», *Eur. Phys. J. C* **77**, 895 (2017), arXiv:1612.07233 [hep-ex]. Updates on http://www.slac.stanford.edu/xorg/hfag

[43] C. Bobeth, A.J. Buras, «Searching for New Physics with $\bar{\mathcal{B}}(B_{s,d} \to \mu\bar{\mu})/\Delta M_{s,d}$», *Acta Phys. Pol. B* **52**, 1189 (2021), arXiv:2104.09521 [hep-ph].

[44] A.J. Buras, E. Venturini, «The exclusive vision of rare K and B decays and of the quark mixing in the standard model», *Eur. Phys. J. C* **82**, 615 (2022), arXiv:2203.11960 [hep-ph].

[45] A.J. Buras, «Standard Model predictions for rare K and B decays without new physics infection», *Eur. Phys. J. C* **83**, 66 (2023), arXiv:2209.03968 [hep-ph].

[46] A.J. Buras, «Hunting new animalcula with rare K and B decays», *EPJ Web Conf.* **314**, 00002 (2024), arXiv:2411.03440 [hep-ph].

[47] A.J. Buras, «Waiting for Precise Measurements of β and γ», arXiv:2305.00021 [hep-ph].

[48] A.J. Buras, «Kaon theory: 50 years later», *Prog. Theor. Exp. Phys.* **2025**, 03A105 (2025), arXiv:2307.15737 [hep-ph].

[49] Fermilab Lattice and MILC collaborations (A. Bazavov *et al.*), «$B^0_{(s)}$-mixing matrix elements from lattice QCD for the Standard Model and beyond», *Phys. Rev. D* **93**, 113016 (2016), arXiv:1602.03560 [hep-lat].

[50] HFLAV Collaboration (Y. Amhis *et al.*), «Averages of b-hadron, c-hadron, and τ-lepton properties as of 2021», *Phys. Rev. D* **107**, 052008 (2023), arXiv:2206.07501 [hep-ex].

[51] LHCb Collaboration (R. Aaij *et al.*), «Measurement of the $B^0_s \to \mu^+\mu^-$ decay properties and search for the $B^0 \to \mu^+\mu^-$ and $B^0_s \to \mu^+\mu^-\gamma$ decays», *Phys. Rev. D* **105**, 012010 (2022), arXiv:2108.09283 [hep-ex].

[52] Belle-II Collaboration (I. Adachi *et al.*), «Evidence for $B^+ \to K^+\nu\bar{\nu}$ decays», *Phys. Rev. D* **109**, 112006 (2024), arXiv:2311.14647 [hep-ex].

[53] Belle Collaboration (J. Grygier *et al.*), «Search for $B \to h\nu\bar{\nu}$ decays with semileptonic tagging at Belle», *Phys. Rev. D* **96**, 091101(R) (2017); *Addendum ibid.* **97**, 099902 (2018), arXiv:1702.03224 [hep-ex].

[54] KOTO Collaboration (J. Ahn *et al.*), «Search for the $K_L \to \pi^0 \nu\bar{\nu}$ and $K_L \to \pi^0 X^0$ decays at the J-PARC KOTO experiment», *Phys. Rev. Lett.* **122**, 021802 (2019), arXiv:1810.09655 [hep-ex].

[55] LHCb Collaboration (R. Aaij *et al.*), «Constraints on the $K^0_S \to \mu^+\mu^-$ Branching Fraction», *Phys. Rev. Lett.* **125**, 231801 (2020), arXiv:2001.10354 [hep-ex].

[56] A.J. Buras, J. Girrbach, «Towards the identification of new physics through quark flavour violating processes», *Rep. Prog. Phys.* **77**, 086201 (2014), arXiv:1306.3775 [hep-ph].

[57] A.J. Buras, «Expedition to the Zeptouniverse», arXiv:2403.02387 [hep-ph].

[58] A.J. Buras, F. De Fazio, J. Girrbach, «The anatomy of Z' and Z with flavour changing neutral currents in the flavour precision era», *J. High Energy Phys.* **2013**, 116 (2013), arXiv:1211.1896 [hep-ph].

[59] A. Buras, «Flavour Expedition to the Zeptouniverse», *PoS* **(FWNP)**, 003 (2015), arXiv:1505.00618 [hep-ph].

[60] A.J. Buras, D. Buttazzo, R. Knegjens, «$K \to \pi\nu\bar{\nu}$ and ε'/ε in simplified new physics models», *J. High Energy Phys.* **2015**, 166 (2015), arXiv:1507.08672 [hep-ph].

[61] C. Albertus *et al.*, «WISPedia — the WISPs Encyclopedia», arXiv:2602.09089 [hep-ph].

[62] W. Altmannshofer, A.J. Buras, D.M. Straub, M. Wick, «New strategies for new physics search in $B \to K^*\nu\bar{\nu}$, $B \to K\nu\bar{\nu}$ and $B \to X_s\nu\bar{\nu}$ decays», *J. High Energy Phys.* **2009**, 022 (2009), arXiv:0902.0160 [hep-ph].

[63] Y. Grossman, Z. Ligeti, E. Nardi, «New limit on inclusive $B \to X_s\nu\bar{\nu}$ decay and constraints on new physics», *Nucl. Phys. B* **465**, 369 (1996); *Erratum ibid.* **480**, 753 (1996).

[64] D. Melikhov, N. Nikitin, S. Simula, «Right-handed currents in rare exclusive $B \to K(K^*)\nu\bar{\nu}$ decays», *Phys. Lett. B* **428**, 171 (1998), arXiv:hep-ph/9803269.

[65] A.J. Buras, J. Girrbach-Noe, C. Niehoff, D.M. Straub, «$B \to K^{(*)}\nu\bar{\nu}$ decays in the Standard Model and beyond», *J. High Energy Phys.* **2015**, 184 (2015), arXiv:1409.4557 [hep-ph].

[66] A.J. Buras, J. Harz, M.A. Mojahed, «Disentangling new physics in $K \to \pi\nu\bar{\nu}$ and $B \to K\,(K^*)\,\nu\bar{\nu}$ observables», *J. High Energy Phys.* **2024**, 87 (2024), arXiv:2405.06742 [hep-ph].

[67] A.J. Buras, F. De Fazio, J. Girrbach-Noe, «Z–Z' mixing and Z-mediated FCNCs in $\mathrm{SU}(3)_C \times \mathrm{SU}(3)_L \times \mathrm{U}(1)_X$ models», *J. High Energy Phys.* **2014**, 039 (2014), arXiv:1405.3850 [hep-ph].

[68] A.J. Buras, P. Stangl, «On the interplay of constraints from from B_s, D, and K meson mixing in Z' models with implications for $b \to s\nu\bar{\nu}$ transitions», *Eur. Phys. J. C* **85**, 519 (2025), arXiv:2412.14254 [hep-ph].

[69] Y. Grossman, Y. Nir, «$K_{\rm L} \to \pi^0 \nu\bar{\nu}$ beyond the Standard Model», *Phys. Lett. B* **398**, 163 (1997), arXiv:hep-ph/9701313.

[70] A.J. Buras, D. Buttazzo, J. Girrbach-Noe, R. Knegjens, «Can we reach the Zeptouniverse with rare K and $B_{s,d}$ decays?», *J. High Energy Phys.* **2014**, 121 (2014), arXiv:1408.0728 [hep-ph].

[71] J. Aebischer, A.J. Buras, J. Kumar, «Kaon physics without new physics in ε_K», *Eur. Phys. J. C* **83**, 368 (2023), arXiv:2302.00013 [hep-ph].

[72] E. Venturini, A.J. Buras, «Standard Model Predictions for Rare K and B Decays without $|V_{cb}|$ and $|V_{ub}|$ Uncertainties*», *PoS* **(CKM2021)**, 094 (2023), arXiv:2203.10099 [hep-ph].

[73] C. Bobeth, A.J. Buras, A. Celis, M. Jung, «Yukawa enhancement of Z-mediated new physics in $\Delta S = 2$ and $\Delta B = 2$ processes», *J. High Energy Phys.* **2017**, 124 (2017), arXiv:1703.04753 [hep-ph].

[74] A.J. Buras *et al.*, «Universal unitarity triangle and physics beyond the standard model», *Phys. Lett. B* **500**, 161 (2001), arXiv:hep-ph/0007085.

[75] A.J. Buras, «Minimal Flavor Violation», *Acta Phys. Pol. B* **34**, 5615 (2003), arXiv:hep-ph/0310208.

[76] M. Blanke, A.J. Buras, D. Guadagnoli, C. Tarantino, «Minimal flavour violation waiting for precise measurements of ΔM_s, $S_{\psi\phi}$, A^s_{SL}, $|V_{ub}|$, γ and $B^0_{s,d} \to \mu^+\mu^-$», *J. High Energy Phys.* **2006**, 003 (2006), arXiv:hep-ph/0604057.

[77] A.J. Buras, J. Girrbach, «On the correlations between flavour observables in minimal U(2)^3 Models», *J. High Energy Phys.* **2013**, 7 (2013), arXiv:1206.3878 [hep-ph].

[78] A.J. Buras, M.V. Carlucci, S. Gori, G. Isidori, «Higgs-mediated FCNCs: natural flavour conservation vs. minimal flavour violation», *J. High Energy Phys.* **2010**, 9 (2010), arXiv:1005.5310 [hep-ph].

[79] A.J. Buras, G. Isidori, P. Paradisi, «EDMs vs. CPV in $B_{s,d}$ mixing in two Higgs doublet models with MFV», *Phys. Lett. B* **694**, 402 (2011), arXiv:1007.5291 [hep-ph].

[80] A.J. Buras, M. Spranger, A. Weiler, «The impact of universal extra dimensions on the unitarity triangle and rare K and B decays», *Nucl. Phys. B* **660**, 225 (2003), arXiv:hep-ph/0212143.

[81] A.J. Buras, A. Poschenrieder, M. Spranger, A. Weiler, «The impact of universal extra dimensions on $B \to X_s\gamma$, $B \to X_s$ gluon, $B \to X_s\mu^+\mu^-$, $K_{\rm L} \to \pi^0 e^+ e^-$ and ε'/ε», *Nucl. Phys. B* **678**, 455 (2004), arXiv:hep-ph/0306158.

[82] A.J. Buras, A. Poschenrieder, S. Uhlig, «Particle–antiparticle mixing, ε_K and the unitarity triangle in the littlest Higgs model», *Nucl. Phys. B* **716**, 173 (2005), arXiv:hep-ph/0410309.

[83] A.J. Buras, A. Poschenrieder, S. Uhlig, W.A. Bardeen, «Rare K and B decays in the littlest higgs model without T-parity», *J. High Energy Phys.* **2006**, 062 (2006), arXiv:hep-ph/0607189.

[84] M. Blanke *et al.*, «FCNC Processes in the Littlest Higgs Model with T-Parity: a 2009 Look», *Acta Phys. Pol. B* **41**, 657 (2010), arXiv:0906.5454 [hep-ph].

[85] I.I. Bigi, M. Blanke, A.J. Buras, S. Recksiegel, «CP violation in D^0–$\bar{D}^0$ oscillations: general considerations and applications to the Littlest Higgs model with T-parity», *J. High Energy Phys.* **2009**, 097 (2009), arXiv:0904.1545 [hep-ph].

[86] M. Blanke, A.J. Buras, S. Recksiegel, «Quark flavour observables in the Littlest Higgs model with T-parity after LHC Run 1», *Eur. Phys. J. C* **76**, 182 (2016), arXiv:1507.06316 [hep-ph].

[87] A.J. Buras *et al.*, «Patterns of flavour violation in the presence of a fourth generation of quarks and leptons», *J. High Energy Phys.* **2010**, 106 (2010), arXiv:1002.2126 [hep-ph].

[88] A.J. Buras *et al.*, «The impact of a 4^{th} generation on mixing and CP violation in the charm system», *J. High Energy Phys.* **2010**, 094 (2010), arXiv:1004.4565 [hep-ph].

[89] A.J. Buras *et al.*, «Lepton flavour violation in the presence of a fourth generation of quarks and leptons», *J. High Energy Phys.* **2010**, 104 (2010), arXiv:1006.5356 [hep-ph].

[90] W. Altmannshofer *et al.*, «Anatomy and phenomenology of FCNC and CPV Effects in SUSY theories», *Nucl. Phys. B* **830**, 17 (2010), arXiv:0909.1333 [hep-ph].

[91] W. Altmannshofer, A.J. Buras, P. Paradisi, «A lower bound on hadronic EDMs from CP Violation in D^0–$\bar{D}^0$ mixing in SUSY alignment models», *Phys. Lett. B* **688**, 202 (2010), arXiv:1001.3835 [hep-ph].

[92] A.J. Buras, M. Nagai, P. Paradisi, «Footprints of SUSY GUTs in flavour physics», *J. High Energy Phys.* **2011**, 5 (2011), arXiv:1011.4853 [hep-ph].

[93] W. Altmannshofer, A.J. Buras, P. Paradisi, «Low energy probes of CP violation in a flavor blind MSSM», *Phys. Lett. B* **669**, 239 (2008), arXiv:0808.0707 [hep-ph].

[94] A.J. Buras, K. Gemmler, G. Isidori, «Quark flavour mixing with right-handed currents: An effective theory approach», *Nucl. Phys. B* **843**, 107 (2011), arXiv:1007.1993 [hep-ph].

[95] M. Blanke *et al.*, «Rare K and B decays in a warped extra dimension with custodial protection», *J. High Energy Phys.* **2009**, 108 (2009), arXiv:0812.3803 [hep-ph].

[96] M. Blanke *et al.*, «$\Delta F = 2$ observables and fine-tuning in a warped extra dimension with custodial protection», *J. High Energy Phys.* **2009**, 001 (2009), arXiv:0809.1073 [hep-ph].

[97] A.J. Buras, J. Girrbach, R. Ziegler, «Particle–antiparticle mixing, CP violation and rare K and B decays in a minimal theory of fermion masses», *J. High Energy Phys.* **2013**, 168 (2013), arXiv:1301.5498 [hep-ph].

[98] A.J. Buras, F. De Fazio, J. Girrbach, M.V. Carlucci, «The anatomy of quark flavour observables in 331 models in the flavour precision era», *J. High Energy Phys.* **2013**, 23 (2013), arXiv:1211.1237 [hep-ph].

[99] A.J. Buras, F. De Fazio, «331 model predictions for rare B and K decays, and $\Delta F = 2$ processes: an update», *J. High Energy Phys.* **2023**, 219 (2023), arXiv:2301.02649 [hep-ph].

[100] A.J. Buras, R. Fleischer, J. Girrbach, R. Knegjens, «Probing new physics with the $B_s \to \mu^+\mu^-$ time-dependent rate», *J. High Energy Phys.* **2013**, 077 (2013), arXiv:1303.3820 [hep-ph].

[101] A.J. Buras *et al.*, «The anatomy of neutral scalars with FCNCs in the flavour precision era», *J. High Energy Phys.* **2013**, 111 (2013), arXiv:1303.3723 [hep-ph].

[102] C. Bobeth, A.J. Buras, «Leptoquarks meet ε'/ε and rare Kaon processes», *J. High Energy Phys.* **2018**, 101 (2018), arXiv:1712.01295 [hep-ph].

[103] C. Bobeth, A.J. Buras, A. Celis, M. Jung, «Patterns of flavour violation in models with vector-like quarks», *J. High Energy Phys.* **2017**, 79 (2017), arXiv:1609.04783 [hep-ph].

[104] R. Bartocci, A. Biekötter, T. Hurth, «Renormalisation group evolution effects on global SMEFT analyses», *J. High Energy Phys.* **2025**, 203 (2025), arXiv:2412.09674 [hep-ph].

[105] F. Feruglio, P. Paradisi, A. Pattori, «Revisiting Lepton Flavor Universality in B Decays», *Phys. Rev. Lett.* **118**, 011801 (2017), arXiv:1606.00524 [hep-ph].

[106] F. Feruglio, P. Paradisi, A. Pattori, «On the importance of electroweak corrections for B anomalies», *J. High Energy Phys.* **2017**, 61 (2017), arXiv:1705.00929 [hep-ph].

[107] J. Aebischer, J. Kumar, «Flavour violating effects of Yukawa running in SMEFT», *J. High Energy Phys.* **2020**, 187 (2020), arXiv:2005.12283 [hep-ph].

[108] L. Allwicher *et al.*, «Computing tools for effective field theories: SMEFT-Tools 2022 Workshop Report, 14–16 September 2022, Zürich», *Eur. Phys. J. C* **84**, 170 (2024), arXiv:2307.08745 [hep-ph].

[109] A.J. Buras, «On the superiority of the $|V_{cb}| - \gamma$ plots over the unitarity triangle plots in the 2020s», *Eur. Phys. J. C* **82**, 612 (2022), arXiv:2204.10337 [hep-ph].

[110] W. Altmannshofer *et al.*, «Symmetries and asymmetries of $B \to K^*\mu^+\mu^-$ decays in the Standard Model and beyond», *J. High Energy Phys.* **2009**, 019 (2009), arXiv:0811.1214 [hep-ph].

[111] A.J. Buras, R. Fleischer, S. Recksiegel, F. Schwab, «$B \to \pi\pi$, New Physics in $B \to \pi K$ and Implications for Rare K and B decays», *Phys. Rev. Lett.* **92**, 101804 (2004), arXiv:hep-ph/0312259.

[112] A.J. Buras, R. Fleischer, S. Recksiegel, F. Schwab, «Anatomy of prominent B and K decays and signatures of CP-violating new physics in the electroweak penguin sector», *Nucl. Phys. B* **697**, 133 (2004), arXiv:hep-ph/0402112.

[113] R. Fleischer, R. Jaarsma, E. Malami, K.K. Vos, «Exploring $B \to \pi\pi, \pi K$ decays at the high-precision frontier», *Eur. Phys. J. C* **78**, 943 (2018), arXiv:1806.08783 [hep-ph].

[114] R. Berthiaume *et al.*, «Anomalies in Hadronic B Decays», *Phys. Rev. Lett.* **133**, 211802 (2024), arXiv:2311.18011 [hep-ph].

[115] A. Datta, J. Kumar, S. Kumbhakar, D. London, «Uniting low-energy semileptonic and hadronic anomalies within SMEFT», *J. High Energy Phys.* **2024**, 175 (2024), arXiv:2408.03380 [hep-ph].

[116] A. Szabelski, «The "$B \to K\pi$ puzzle": a new perspective», *Eur. Phys. J. C* **84**, 1319 (2024), arXiv:2410.16396 [hep-ph].